Extreme Anomalous Atmospheric Circulation in the West Antarctic Peninsula Region in Austral Spring and Summer 2001/02, and Its Profound Impact on Sea Ice and Biota*

ROBERT A. MASSOM,[a] SHARON E. STAMMERJOHN,[b] RAYMOND C. SMITH,[c] MICHAEL J. POOK,[d] RICHARD A. IANNUZZI,[b] NEIL ADAMS,[e] DOUGLAS G. MARTINSON,[b] MARIA VERNET,[f] WILLIAM R. FRASER,[g] LANGDON B. QUETIN,[h] ROBIN M. ROSS,[h] YUKO MASSOM,[i] AND H. ROY KROUSE[j]

[a] *Department of the Environment and Heritage, Australian Antarctic Division, and Antarctic Climate and Ecosystems Cooperative Research Centre, University of Tasmania, Hobart, Tasmania, Australia*
[b] *Lamont-Doherty Earth Observatory, Columbia University, Palisades, New York*
[c] *ICESS, and Department of Geography, University of California, Santa Barbara, Santa Barbara, California*
[d] *CSIRO Division of Marine and Atmospheric Research, Hobart, Tasmania, Australia*
[e] *Australian Bureau of Meteorology, and Antarctic Climate and Ecosystems Cooperative Research Centre, University of Tasmania, Hobart, Tasmania, Australia*
[f] *Integrative Oceanographic Division, Scripps Institution of Oceanography, University of California, San Diego, La Jolla, California*
[g] *Polar Oceans Research Group, Sheridan, Montana*
[h] *Marine Science Institute, University of California, Santa Barbara, Santa Barbara, California*
[i] *National Oceans Office, Hobart, Tasmania, Australia*
[j] *Department of Physics and Astronomy, University of Calgary, Calgary, Alberta, Canada*

(Manuscript received 12 April 2005, in final form 3 October 2005)

ABSTRACT

Exceptional sea ice conditions occurred in the West Antarctic Peninsula (WAP) region from September 2001 to February 2002, resulting from a strongly positive atmospheric pressure anomaly in the South Atlantic coupled with strong negative anomalies in the Bellingshausen–Amundsen and southwest Weddell Seas. This created a strong and persistent north-northwesterly flow of mild and moist air across the WAP. In situ, satellite, and NCEP–NCAR Reanalysis (NNR) data are used to examine the profound and complex impact on regional sea ice, oceanography, and biota. Extensive sea ice melt, leading to an ocean mixed layer freshening and widespread ice surface flooding, snow–ice formation, and phytoplankton growth, coincided with extreme ice deformation and dynamic thickening. Sea ice dynamics were crucial to the development of an unusually early and rapid (short) retreat season (negative ice extent anomaly). Strong winds with a dominant northerly component created an unusually compact marginal ice zone and a major increase in ice thickness by deformation and over-rafting. This led to the atypical persistence of highly compact coastal ice through summer. Ecological effects were both positive and negative, the latter including an impact on the growth rate of larval Antarctic krill and the largest recorded between-season breeding population decrease and lowest reproductive success in a 30-yr Adélie penguin demographic time series. The unusual sea ice and snow cover conditions also contributed to the formation of a major phytoplankton bloom. Unexpectedly, the initial bloom occurred within compact sea ice and could not be detected in Sea-Viewing Wide Field-of-View Sensor (SeaWiFS) ocean color data. This analysis demonstrates that sea ice extent alone is an inadequate descriptor of the regional sea ice state/conditions, from both a climatic and ecological perspective; further information is required on thickness and dynamics/deformation.

* Supplemental information related to this paper is available at the Journals Online Web site: http://dx.doi.org/10.1175/JCLI3805.s1.

Corresponding author address: Rob Massom, Antarctic Climate and Ecosystems Cooperative Research Centre, University of Tasmania, Private Bag 80, Hobart, Tasmania 7001, Australia.
E-mail: R.Massom@acecrc.org.au

© 2006 American Meteorological Society

1. Introduction

The West Antarctic Peninsula (WAP) is under close scrutiny as a region of high climate sensitivity. No other part of the Southern Hemisphere has experienced such a rapid warming trend over the past half-century, of fully 0.5°C per decade (King 1994; King and Comiso 2003; King and Harangozo 1998; Smith et al. 1996; Vaughan et al. 2001). Moreover, the WAP and adjoining southern Bellingshausen Sea regions are the only Antarctic sectors to have undergone a statistically significant decrease in sea ice extent over the past few decades, that is, over the era when satellite passive-microwave data have been available (Stammerjohn and Smith 1997; Zwally et al. 2002). This trend has resulted from a decrease in the duration (but not extent) of sea ice maximum extent (Smith and Stammerjohn 2001; see also Parkinson 2002). It has been proposed that the long-term warming trend is associated with changes in sea ice area extent in the Bellingshausen Sea, as fluctuations in the latter correlate strongly with variations in austral winter air temperatures along the WAP (Jacobs and Comiso 1997; Smith et al. 2003b). Stammerjohn and Smith (1996) provide a detailed discussion of sea ice characteristics and variability in the region. Evidence has emerged that with the recent shortening of the regional sea ice duration, there has been an apparent gradual replacement of the continental, polar regime characteristic of the southern WAP with a more maritime and warmer regime characteristic of the northern WAP (Smith et al. 2003b). Ecosystem responses sensitive to sea ice changes are becoming increasingly apparent (Chapman et al. 2004; Fraser and Hofmann 2003; Ross et al. 1996; Smith et al. 1999; Smith et al. 2003a).

Evidence is also emerging of significant cyclical behavior in atmospheric circulation anomalies over the Southern Ocean—over a range of spatiotemporal scales and with teleconnections to lower-latitude phenomena (Carleton 2003; Liu et al. 2002a,b; White et al. 2002; Yuan and Martinson 2000). Major patterns include the Semi-Annual Oscillation (Enomoto and Ohmura 1990; Meehl et al. 1998; Simmonds 2003; Van den Broecke 1998), El Niño/La Niña (Carleton 2003; Gloersen 1995; Harangozo 2000; Kwok and Comiso 2002a,b; Simmonds and Jacka 1995; Smith and Stammerjohn 2001; Turner 2004; Yuan 2004), and the circumpolar propagation of coupled atmospheric–oceanic anomalies within the Antarctic Circumpolar Wave (Connolley 2003; White and Peterson 1996). On the decadal scale, recent change has been observed in large-scale tropospheric circulation in the form of a strengthening and contraction of the circumpolar vortex, and concomitant strengthening of the circumpolar westerlies (Gillett and Thompson 2003; Hurrell and van Loon 1994; Thompson and Solomon 2002). This is associated with the so-called Southern Annular Mode (SAM), or Antarctic Oscillation (Fyfe et al. 1999; Hall and Visbeck 2002; Karoly 1990; Kidson 1988; Raphael 2003; Thompson and Wallace 2000). The SAM is the dominant pattern of atmospheric variability in the Southern Hemisphere. According to Turner et al. (2004), localized factors have also played a role in the recent weather and climate of the Antarctic Peninsula region. Other dominant patterns of variability include the Pacific–South American mode and the Antarctic Dipole described by Yuan and Martinson (2001), which entails atmospheric anomalies of opposite sign in the southwest Atlantic and southeast Pacific Oceans. Carleton (2003), Simmonds (2003), and Simmonds and King (2004) provide in-depth reviews of modes of variability in the Southern Hemisphere atmosphere.

In this paper, we report upon exceptional atmospheric and resultant extreme sea ice conditions encountered during and after research cruise NBP01–5 on the R/V *Nathaniel B. Palmer* to the Bellingshausen Sea in the late winter to early spring of 2001. The study region and cruise track are shown in Fig. 1. The ice phase of the cruise lasted from 11 September to 22 October 2001. This cruise was carried out as part of the U.S. National Science Foundation's Palmer Long-Term Ecological Research (LTER) program, the overall aim of which is to understand the structure and function of the Antarctic marine ecosystem in response to variability in oceanic, atmospheric, and sea ice forcing (Smith et al. 1995, 2003b; Ross et al. 1996; http://www.icess.ucsb.edu/lter/lter.html).

We show that the protracted anomalous sea ice conditions first encountered in the Bellingshausen Sea in late 2001 persisted through the austral summer of 2001/02 and resulted from large-scale anomalies in atmospheric circulation. We then assess the profound impact of the anomalous atmospheric circulation on regional (i) sea ice and snow cover melt and ice microstructure, (ii) upper-ocean structure, (iii) sea ice dynamics, (iv) sea ice concentration and extent, and (v) ice and snow thickness distributions. An assessment is then made of the resultant impacts on sea ice biota and the subsequent ecological impact (both positive and negative) of these unusual conditions. Finally, the regional conditions are examined in the context of wider patterns of anomalous atmospheric circulation. This paper complements that of Turner et al. (2002), who examined the impact of this anomalous atmospheric circulation pattern in creating unusually heavy ice conditions in the eastern Weddell Sea in early 2002. General sea ice con-

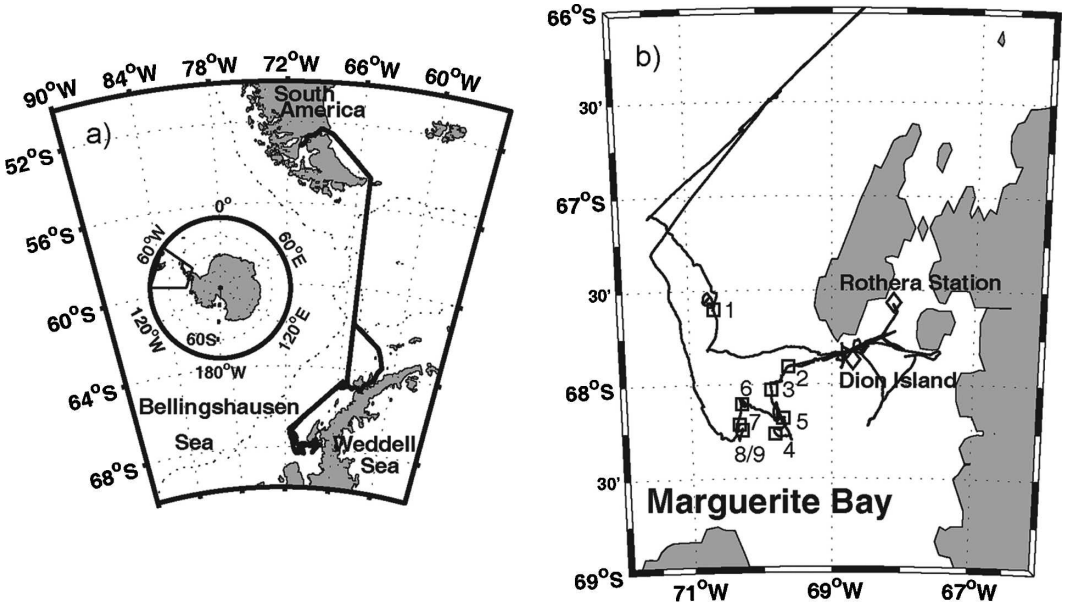

FIG. 1. (a) Map of the study region, showing the cruise track voyage NBP01–05 of the R/V *Nathaniel B. Palmer*. (b) Enlarged map is of the Marguerite Bay region, showing the cruise track with ice stations marked. The BAS Rothera Station is located on the southeast coast of Adelaide Island. Dates for the station numbers are as follows: 1) 15–17 Sep; 2) 21 Sep; 3) 26–27 Sep; 4) 30 Sep; 5) 3 Oct; 6) 6 Oct; 7) 8 Oct; 8) 11 Oct; and 9) 14 Oct (all 2001).

ditions in the region over the period leading up to the anomaly (i.e., the austral winter of 2001) are described by Perovich et al. (2004), and regional water mass characteristics are described by Klinck et al. (2004).

2. Data and techniques

Data from various sources were used in this analysis. The first comprises in situ data collected during the cruise. Detailed analysis was carried out on the physical properties of sea ice core and snow cover samples. Many of these were collected within Marguerite Bay (see the ice stations marked on Fig. 1), where the ship became beset for nearly two weeks. The relative contribution of the meteoric component of the ice cores (i.e., snow–ice) was determined by oxygen isotope ($\delta^{18}O$) analysis of ice core samples and by crystallographic analysis of vertical thin sections under polarized light. Because of the extreme ice thicknesses encountered, the core samples are primarily from the upper few meters of the ice cover only. This cover typically comprised a number of rafted blocks with an individual thickness of ~0.5–1.0 m, and separated by water-filled interstices, which were centimeters to tens of centimeters wide. Observations of ice thickness and under-ice structure were acquired by scuba divers equipped with underwater video cameras. Oceanographic data from an onboard conductivity–temperature–density (CTD) sampling program were used to determine changes in the water column characteristics related to surface melt. The experiment also included a detailed program to measure biomass, primary production, and nutrient concentration both in the ice and water column; this was carried out in tandem with the sea ice and oceanographic programs. Meteorological conditions were analyzed using (i) data collected on the ship and (ii) 12-hourly maps of mean sea level pressure (MSLP) and 500-hPa geopotential height data from the National Centers for Environmental Prediction–National Center for Atmospheric Research (NCEP–NCAR) Reanalysis (NNR) project (Kalnay et al. 1996)—the latter to spatiotemporally extend the direct observations. Wind velocity data were computed from 10-m zonal and meridional monthly mean winds from the NNR dataset. These data are in equal-area format, with a grid size of ~1.89° (meridional) by 1.875° (zonal). Monthly wind field anomalies were computed using monthly means for the period 1980–2001. No NNR data are used before 1979 because of their unreliability prior to this date (Hines et al. 2000; Marshall and Harangozo 2000). Meteorological data collected at Rothera Station in Marguerite Bay (ID 89062, 67.51°S, 68.1°W) were used to verify patterns observed in NNR analysis outside the period of direct surface observations made during the cruise, that is, from late October 2001 to February 2002 inclusive. (Information on the

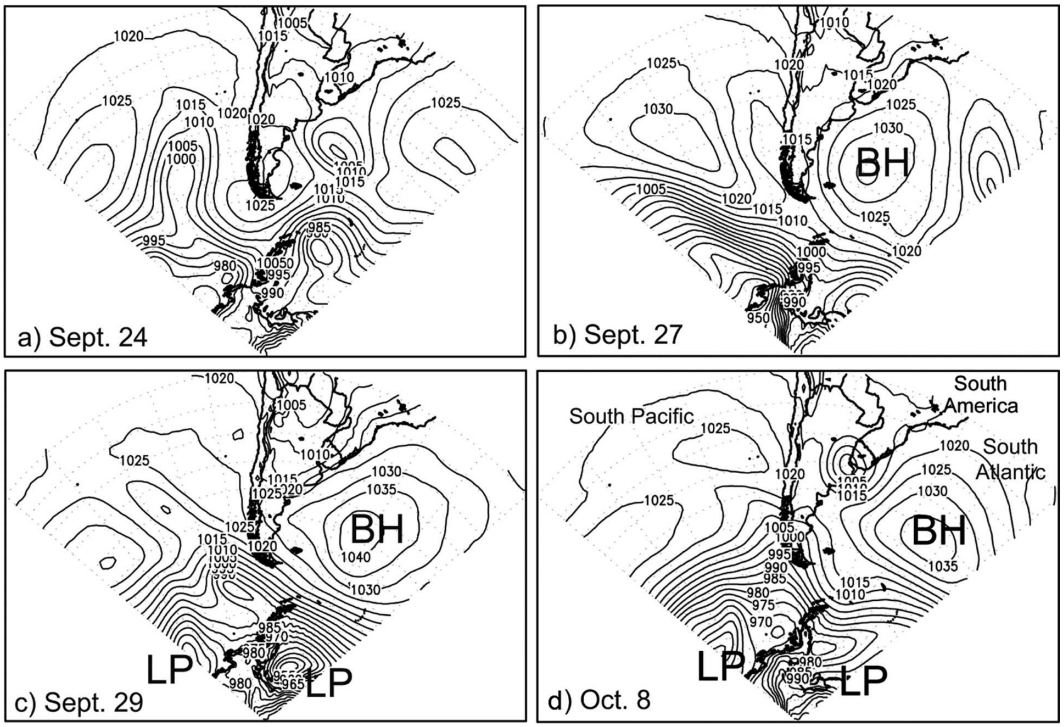

FIG. 2. Synoptic charts of NNR MSLP in the South Pacific, South Atlantic, and Antarctic Peninsula region at 2300 UTC on (a) 24, (b) 27, and (c) 29 Sep 2001 and (d) 8 Oct 2001, showing the initial establishment of the blocking high in the South Atlantic and the deep low pressure centers in the Amundsen–Bellingshausen and western Weddell Seas. Note the resultant strong northwest-to-southeast alignment and close spacing of isobars in the WAP region. Pressure values are in hPa.

monthly SAM index was obtained from the British Antarctic Survey online at http://www.nerc-bas.ac.uk/icd/gjma/sam.html.)

In situ growth experiments were carried out with larval Antarctic krill (*Euphausia superba*), in a manner described in detail in Quetin et al. (2003) and Ross et al. (2004) and using scuba diving. Chlorophyll samples were also taken to estimate biomass, that is, ice algae and phytoplankton standing stocks. Chlorophyll was measured using a Turner Designs digital 10-AU-05 fluorometer, calibrated using a chlorophyll *a* (chl *a*) standard from Sigma Chemicals. Water aliquots were collected using Niskin bottles attached to a CTD rosette, filtered onto HA Millipore filters (0.45 microns pore size) under vacuum and extracted for 24 h in 10 ml of 90% acetone (Smith et al. 1981). A similar procedure was used for the ice samples. Ice cores were cut into 5-, 10-, or 20-cm sections, then melted in containers in the dark at room temperature and filtered immediately after the sample was completely melted and at a temperature of about 2° or 3°C. Once again, ice cores for biological sampling were only collected from the upper few meters of the ice, given the extreme over-rafted ice thickness. Water aliquots for the measurement of nutrient concentrations were sampled in a similar fashion to the chlorophylls and analyzed within 12 h of sampling. Silicic acid [Si(OH)2-], orthophosphate (PO4-), nitrate (NO3-), and ammonium (NH4+) concentrations were measured according to the methods described in Johnson et al. (1985), using a Perstorp/Alpken segmented-flow nutrient analysis system and Labtronics data collection software.

Satellite data extend the analysis both spatially and temporally. Daily maps of sea ice concentration and extent (pixel size 25 × 25 km) were derived from brightness temperature data from the Defense Meteorological Satellite Program (DMSP) Special Sensor Microwave Imager (SSM/I; 1987–present) and Nimbus 7 Scanning Multichannel Microwave Radiometer (SMMR; 1978–1987), using the National Aeronautics and Space Administration (NASA) Bootstrap algorithm (Comiso 1995). Initial analysis also included maps of monthly averaged ice motion derived from SSM/I satellite data using the technique of Emery et al. (1997). Cloud patterns and sea ice distributions were analyzed using visible and thermal infrared data from the NOAA Advanced Very High Resolution Radiometer (AVHRR; ~1-km resolution) and the DMSP Op-

erational Linescan System (OLS; 0.55–2.7-km resolution). These data were collected onboard the R/V *Nathaniel B. Palmer* using a SeaSpace TeraScan system. Also, cloud patterns were analyzed using Antarctic 3-hourly composite images comprising NOAA AVHRR and geostationary satellite data from the University of Wisconsin Space Science and Engineering Center (http://www.ssec.wisc.edu/data/composites.html).

Regional maps of the upper-ocean chlorophyll concentration were estimated from ocean color satellite data from the Sea-Viewing Wide Field-of-View Sensor (SeaWiFS). The data used were Global Area Coverage (GAC) standard mapped data, derived by applying the OC4V4 algorithm (O'Reilly et al. 1998) and averaged over the months October 2001 to January 2002 inclusively using the maximum likelihood estimator mean. The pixel resolution is 9.77 km in the nort–south direction and 4.2 km in the east–west direction in the area of interest. For further details, see Dierssen and Smith (2000) and R. C. Smith et al. (2006, unpublished manuscript).

3. Anomalous atmospheric circulation in late 2001–early 2002

The initial establishment (onset) of a blocking-high pattern centered on ~50°S, 35°W in the South Atlantic in late September 2001 is depicted in Fig. 2. A blocking high is an anticyclone that remains quasi-stationary for several days in the midlatitudes where zonal flow usually prevails and the frequent passage of cyclones is the norm. Various objective definitions of the phenomenon have been developed for the Southern Hemisphere (e.g., van Loon 1956; Lejenäs 1984; Trenberth and Mo 1985; Sinclair 1996; Wright 1974). While the South Atlantic is a common location for blocking-high activity (Sinclair 1996), with a concomitant impact on sea ice extent (Harangozo 1997), the late 2001 pattern was highly atypical both in terms of its magnitude and persistence. Indeed, it persisted from September 2001 to February 2002 to dominate the regional meteorology, as shown in the monthly mean composite anomaly map of Southern Hemisphere 500-hPa geopotential height over the period 1980–2001 (Fig. 3). Key features in the hemispheric map are (i) an amplified wavenumber-3 pattern in the Southern Ocean coupled with (ii) deep low pressure (negative) anomalies of –150 gpm in the Bellingshausen–Amundsen Seas and –135 gpm in the southwest Weddell Sea. The largest high pressure (positive) anomaly (of >150 gpm) was located in the South Atlantic. The extreme nature of this anomalous pattern is indicated by the fact that the high pressure recorded at South Georgia (~54.5°S, 37°W) was four

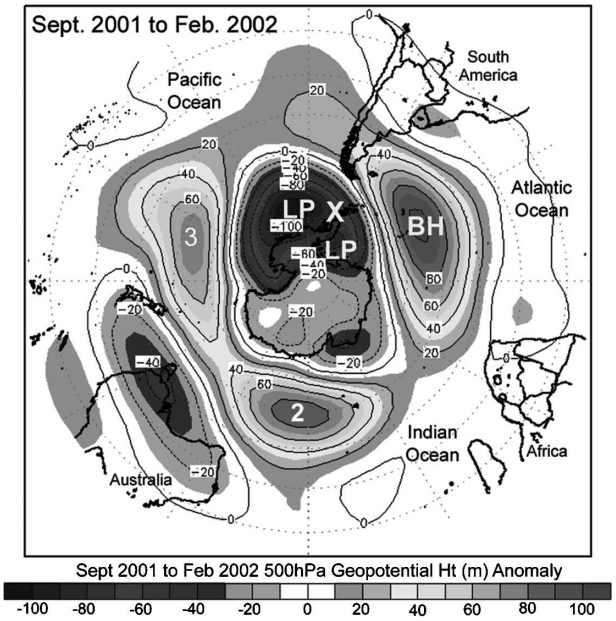

FIG. 3. Monthly mean composite anomaly map of NNR 500-hPa geopotential height for the Southern Ocean and Antarctica for September 2001 to February 2002 (based upon the mean September to February 1980–2001). Here X is the approximate location of Marguerite Bay and the 2001 field experiment, and BH and LP denote the high pressure (positive or blocking-high) and low pressure (negative) anomalies, respectively.

standard deviations above the 1971–2000 mean and represented a one-in-a-century event according to Turner et al. (2002). As stated by the latter, these negative anomalies were substantially different from the typical "Antarctic Dipole" regional pattern of atmospheric circulation (Yuan and Martinson 2001).

The anomalous pattern shown in Fig. 3 bears some resemblance to the SAM, as represented by the first mode of variability in principal component analysis of the hemispheric atmospheric pressure field (Simmonds and King 2004; Thompson and Wallace 2000; Thompson and Solomon 2002; Hall and Visbeck 2002). This dominant mode of variability is characterized by a wavenumber-3 pattern, that is, zonal asymmetry [please see Kidson (1999) and Raphael (2003) for further information on this type of pattern]. In recent decades, the SAM has assumed an increasingly positive polarity (Simmonds and Keay 2000; Thompson et al. 2000), leading to a strengthening of the westerly wind field (Liu et al. 2004). According to the British Antarctic Survey (BAS) SAM index, the effects of a positive SAM event were indeed experienced over the period September 2001 through February 2002 (with monthly values of 0.93, 1.36, 2.14, 1.17, 2.11, and 2.79, respectively). What is notable about conditions in 2001/02,

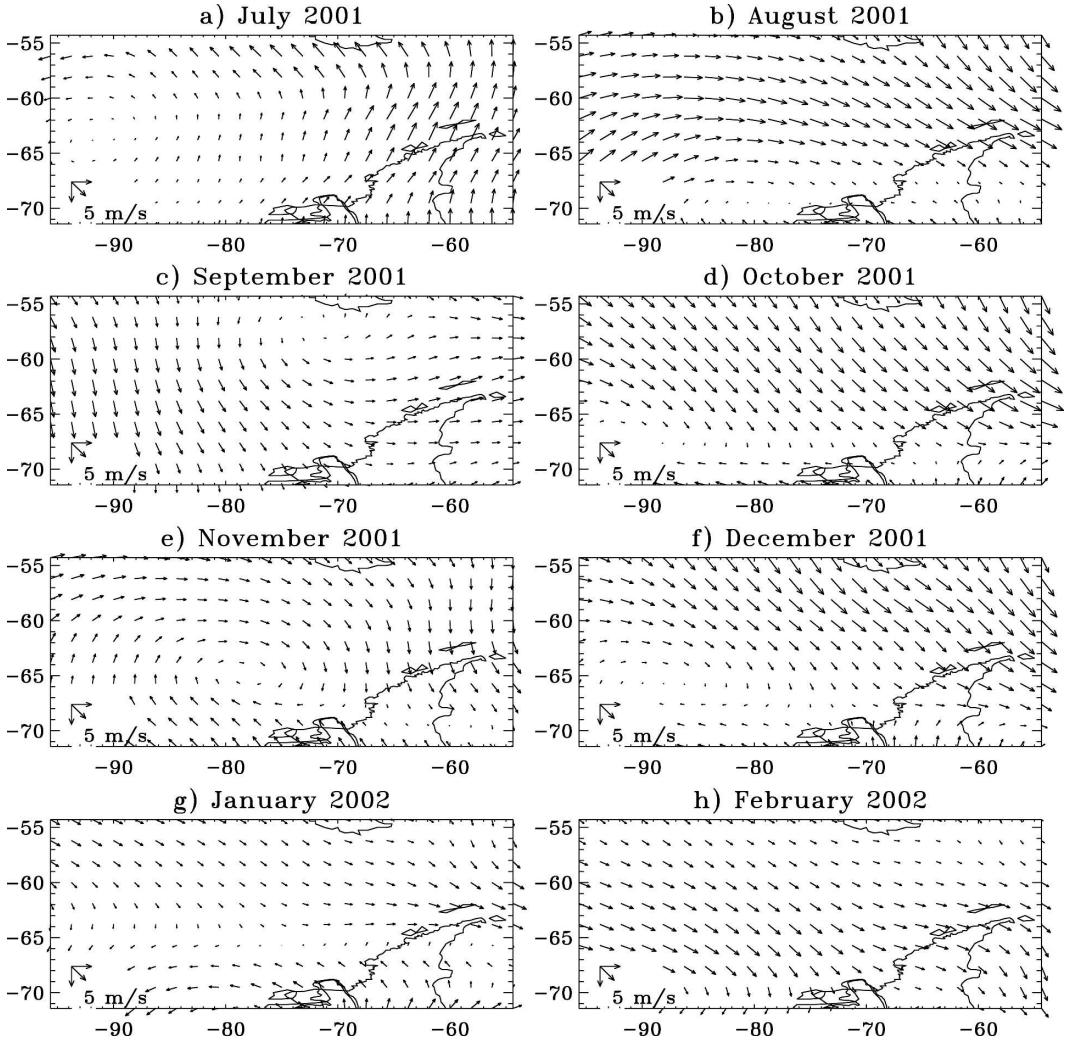

FIG. 4. Anomaly maps of monthly mean 10-m wind fields for July 2001–February 2002, for the WAP region, derived from monthly mean NCEP–NCAR reanalysis project data from 1980 to 2001 inclusive. A wind vector arrow scale is provided in the bottom left of each panel.

and described here, is the deepening of the negative-pressure anomalies to the south of the South Atlantic blocking high, that is, centered on the Amundsen–Bellingshausen Seas and the western Weddell Sea. The net effect was a significant increase in the surface pressure gradient between South Georgia and the Antarctic Peninsula, setting up a strong predominantly northwesterly airflow across the WAP.

Under more "normal" circumstances, the WAP region experiences prevailing westerly winds, with high synoptic-scale variability (King and Turner 1997; Smith et al. 1996). An analysis of the mean-monthly climatological 10-m wind field derived from NNR data for August through February over the period 1980–2001 (not shown) indicates that the near-shore region of the WAP, and including Marguerite Bay, exhibits something of a northwesterly component with speeds of <10 m s^{-1}. This changes to more of a westerly component offshore. An exceptional departure from the climatological mean occurred from September 2001 through February 2002, however, as shown in Fig. 4 (an anomaly map of monthly mean wind speed and direction based on data from 1980–2001 inclusive). The near-surface winds over this period are remarkable in their directional constancy, that is, from the north-northwest, and their strength (>10 m s^{-1}), and also over a broad band extending across the Bellingshausen Sea and Drake Passage.

The overriding impact of the anomalous atmospheric pattern on the regional meteorology is confirmed in the time series of measurements collected at the ship, in the Marguerite Bay region, for the period 11 September–

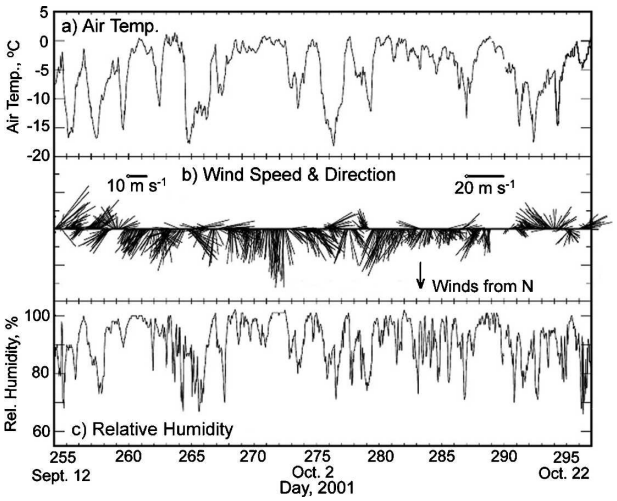

FIG. 5. Time series plots of (a) air temperature, (b) wind speed and direction, and (c) relative humidity measured at the R/V *Nathaniel B. Palmer* while in the Bellingshausen Sea ice zone, 11 Sep to 24 Oct 2001. These are hourly averages of data collected every minute.

24 October (Fig. 5), that is, the onset and early part of the anomalous phase. Strong winds (in excess of 20 m s^{-1}) with a predominantly northerly component persisted over a long period, resulting in the transport of relatively warm and moist air of mid/low-latitude origin across the Bellingshausen Sea ice zone. While strong northerly winds are common in this region over 1–2-week periods and associated with storms (Stammerjohn et al. 2003; Turner et al. 2003), the 2001/02 case was extraordinary in its duration. Analysis of cloud patterns in satellite image time series (not shown) confirm that this air originated from as far north as ~30°S in the South Pacific Ocean (Fig. SM1 in supplementary material online at http://dx.doi.org/10.1175/JCLI3805.s1). This warm moist airflow from the north-northwest resulted in persistent periods of high surface air temperatures (of −1° to +1°C). The longer-term dominance of a warm northerly airstream (from September 2001 through February 2002) is confirmed in contemporary surface meteorological data from Rothera Station. Comparison of average air temperatures from the austral spring through summer of 2001/02 with those from 1977–2004 shows (Table 1) that temperatures were significantly warmer over the springtime of 2001 compared to the long-term average, that is, −3.43° ± 3.67°C versus –5.59° ± 5.94°C. The summertime means of 2001/02 and 1977–2004, on the other hand, were very similar (at 0.86° ± 1.57°C and 0.87° ± 1.868°C, respectively).

The anomalous persistence of the blocking-high pattern in the South Atlantic in 2001/02 is confirmed by the application of an objective atmospheric blocking index (BI). In this case, and following Pook and Gibson (1999),

$$\mathrm{BI} = 0.5(u_{25} + u_{30} + \underline{u}_{55} + u_{60} - u_{40} - u_{50} - 2u_{45}), \quad (1)$$

where u_x is the zonal (westerly) component of the wind speed (m s^{-1}) at the 500-hPa atmospheric level at latitude x. Positive (negative) values of the index result when the westerly or zonal flow is weak (strong) at midlatitudes and well (poorly) developed at low and high latitudes. In other words, positive anomalies represent a tendency toward blocking.

We have computed the BI from NNR data to obtain an anomaly along the 30°W meridian in each October relative to the mean October value for the period 1980–2001 inclusive. The results presented in Fig. 6a show that the value of the blocking index anomaly (BIA) at 30°W in October 2001 was, at more than 1.5 standard deviations from the mean, the highest positive in the 21-yr record. Similarly, the BIA time series for the austral spring (September–November), shown in Fig. 6b, demonstrates that the positive 2001 BI anomaly was also the strongest since 1989 (note that a high BIA also occurred in 1987). Also shown, in Fig. 6c, is the BIA time series for the austral summer (December–February). In this case, the "year" of the particular summer refers to the year in which the austral summer period ended. Once again, a strong BIA is apparent for the austral summer of 2002 (marked A) and is more than two standard deviations above the mean. Note that the summer ending in February 2000 also exhibits a signifi-

TABLE 1. The average, one std dev (1σ), maximum and minimum of surface air temperature data collected at Rothera Station (ID 89062; 67.51°S, 68.1°W), comparing data from the austral spring through summer of 2001/02 with the long-term average from 1977 to 2004. The austral spring is September–November (SON) and the austral summer is December–February (DJF).

	Sep 2001	Sep 1977–2004	Oct 2001	Oct 1977–2004	Nov 2001	Nov 1977–2004	SON 2001	SON 1977–2004	DJF 2001/02	DJF 1977–2004
Average, °C	−5.12	−8.82	−3.25	−5.802	−1.83	−2.15	−3.43	−5.59	0.86	0.87
1σ	4.72	7.07	2.72	4.97	2.12	3.03	3.67	5.94	1.57	1.87
n	720	10,409	656	10,668	685	10,406	2061	31,483	2089	30,084
Max	3.60	3.60	2.60	4.50	2.40	6.80	3.60	6.80	6.3	8.70
Min	−15.70	−38.20	−10.3	−31.10	−7.90	−20.50	−15.7	−38.20	−3.6	−11.00

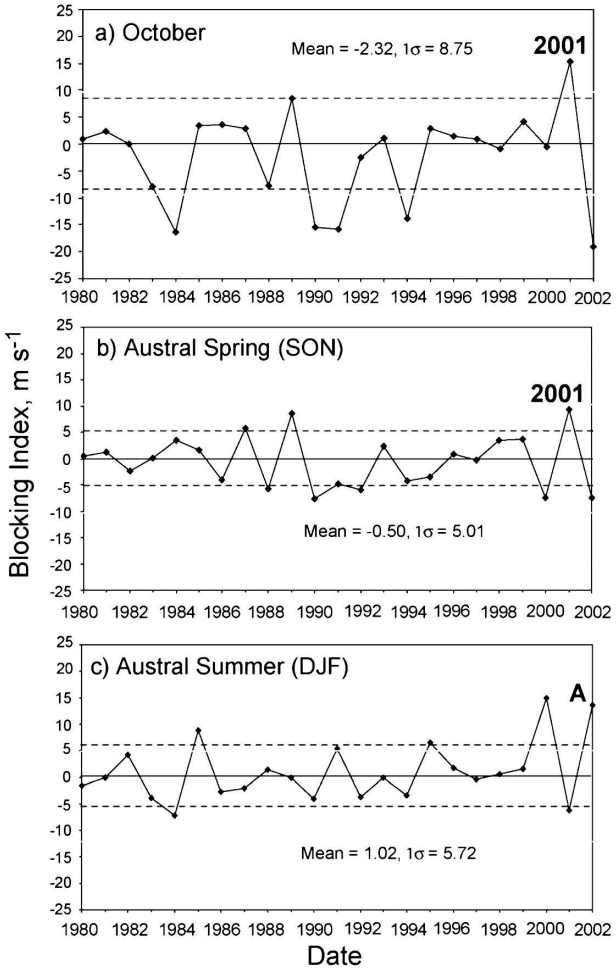

FIG. 6. Time series plot of the BIA at 30°W from 1980 to 2001 inclusive for (a) October, (b) the austral spring (SON inclusive), and (c) the austral summer (DJF inclusive). These data were derived from monthly mean values from the NNR dataset. In (c), A marks the high BIA in the summer of 2001/02. The dashed lines signify ±1 std dev (±1σ).

cant blocking anomaly. Only 1985/86 exhibits an anomaly that is in any way comparable to the 2001/02 and 1999/2000 events. In all cases (i.e., October, spring, and summer), the strong anomaly reported here is preceded and/or followed by strong BIA values of the opposite sign.

The anomalous nature of the 2001/02 event is further confirmed through analysis of NNR-derived monthly mean meteorological variables at 850 hPa from 65°S, 70°W (in the vicinity of Marguerite Bay). Data from 1979–2002 are shown in Fig. 7. Certain years, such as 1981/82, 1993/94, and 1999/2000, exhibit unusual constancy in wind direction from the north/northwest. The 2001/02 event alone, however, is notable not only for a predominantly northerly airflow but also for the relative constancy of strong winds and the advection of low-latitude air masses with high moisture content meridionally across the WAP sea ice zone (1983 exhibits similar characteristics, but a lower wind speed). Specifically, Fig. 7e depicts monthly mean precipitation rates. It shows that the peak in late 2001 was unusual over the last decade, with precipitation rates exceeding 5.5 mm day^{-1} (water equivalent) over a prolonged period.

4. Profound impact on the regional sea ice cover

The profound impact on sea ice conditions in the WAP region was both complex and paradoxical, and was felt over a wide range of scales—from micro to regional. In this section, we examine the net effect on sea ice and snow cover properties, extent and thickness, and the underlying ocean structure.

a. Widespread sea ice and snow cover melt

The prolonged incursion of warm air caused widespread unseasonable melt of both the ice and its snow cover. The ice cover was typically warm and isothermal, with vertical temperature profiles through the upper few meters of the ice showing values on the order of −1.6° to −1.8°C during prolonged warm spells. Analysis of core samples revealed the considerable impact on sea ice microstructure and properties. An example core, collected on 26 September (about 3 days after the onset of the atmosphere anomaly; see Fig. 2), is shown in Fig. SM2. The air temperature at this time was −1.4°C, with strong (20 m s^{-1}) northerly winds. The upper 30% (~15 cm) of these ice cores comprised opaque and semiconsolidated slushy horizons, indicating incorporation of snow into the sea ice matrix (as confirmed by subsequent thin section and δ^{18}O analysis). Separated by a horizon of slushy melt voids, the ice below this was harder, but characterized by significant melt in the form of enlarged brine channels, in this case ~1–2 cm in diameter, rendering the ice highly porous. Golden et al. (1998) show that sea ice with a salinity of 5 psu becomes porous and its brine volume large once its temperature exceeds ~−5°C. Both of these thresholds (collectively termed the percolation threshold) were greatly exceeded for long periods (see also Perovich et al. 2004). This has important implications in that the enlarged brine channels coalesce to allow the downward transport of meltwater and/or the upward incursion of seawater (and macronutrients and algae) through the ice matrix and onto the snow–ice interface.

Similarly, snow cover properties were dominated by melt characteristics in upper horizons, for example, crystal enlargement and rounding and the creation of icy melt layers (Colbeck 1982), and by saturation of the lower layers by seawater flooding to form slush. Intermediate layers were themselves dampened and affected

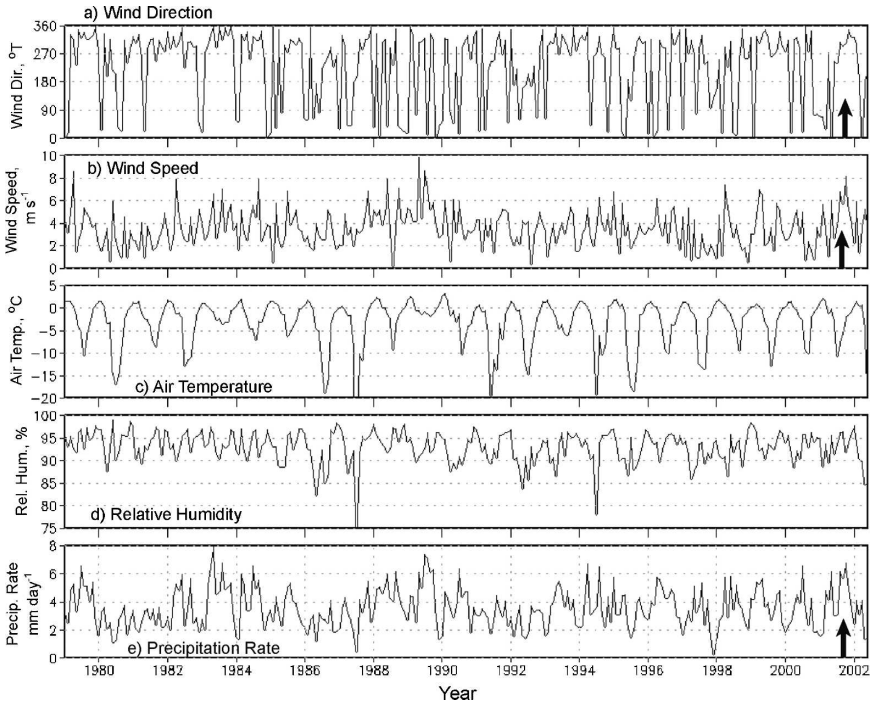

FIG. 7. Time series of meteorological variables at a height of 850 hPa and at 65°S, 70°W (in the vicinity of Marguerite Bay), computed from NNR data for the period 1979–2002. Monthly mean values are plotted for (a) wind direction, (b) wind speed, (c) air temperature, (d) relative humidity, and (e) precipitation rate. The arrows highlight the period of interest.

by the upward capillary "wicking" of brine from the slush horizon, in the manner described by Massom et al. (2001). This led to dampness, salinities of >10 psu, and significant snow metamorphism (i.e., crystal rounding and enlargement). Even in the absence of flooding, the lower snow layers were typically damp and saline. Snow salination in this manner affects the melt characteristics of the surface in response to high air temperatures, that is, a saline snow melts at a lower temperature than a fresh snow layer.

In spite of the prevailing high temperatures, the base of the individual rafted blocks comprising the floes (see section 4.4) was typically characterized by apparent sea ice growth, in the form of a layer of dendritic crystals 1.5–2.0 cm in length and protruding vertically downward. Why basal ice growth should occur contemporaneously with significant melt above is unknown. It may relate, however, to the existence of a sheltered "microclimate" of lower salinity water lenses at the base of floes and in the ~10-cm-wide seawater-filled interstitial gaps between the rafted-floe layers. These lenses, termed "under-ice melt ponds" in the Arctic by Hanson (1965), result from the release of meltwater percolating downward through the overlying ice. This lower-salinity meltwater would refreeze on contact with the colder ocean (at a temperature of approximately –1.8°C). Because of the lower salinity of the under-ice melt pools, its temperature is below the melting point of the dendrites. This basal growth under melt conditions may be the equivalent of so-called "false bottoms" observed in the Arctic sea ice in summer (Eicken et al. 2002; Hanson 1965; Notz et al. 2003). That basal growth occurred at a time of melt is borne out by oxygen-isotope analysis of ice cores cut into 10-cm samples. Compared to seawater, Antarctic snow is relatively depleted in the heavy stable isotope, ^{18}O, and therefore has a significant negative $\delta^{18}O$ value (Eicken 1998; Jeffries et al. 1994a, 1998). The $\delta^{18}O$ values measured from the basal strata in 2001 ranged from ~−0.2 to −18 ppm. Work in the Arctic has shown that "redistribution" of meltwater in this fashion has important implications for both the ice mass balance (Eicken et al. 2002) and the salt and heat balance of the ocean mixed layer (Kadko 2000).

b. Significant freshening of the ocean mixed layer

The persistent melt described above led to noticeable freshening of the upper ocean in the early austral spring of 2001. Figure 8 presents CTD data from two downcasts (vertical profiles) at roughly the same location (~3 km apart due to ship drift) in Marguerite Bay (at

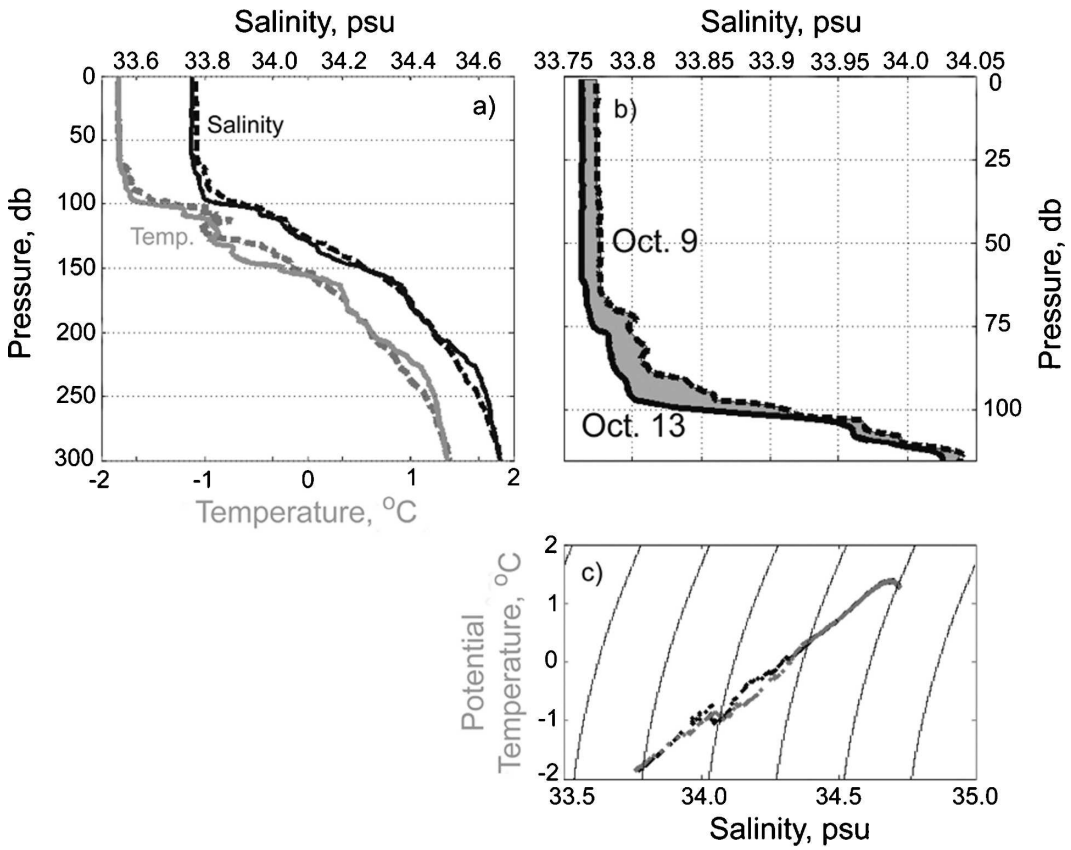

FIG. 8. CTD data from 9 and 13 Oct 2001, in Marguerite Bay (at ~68°S, 70°W). (a) Temperature and salinity (*T/S*) profiles of the upper ocean; (b) a close-up of the salinity profiles across the approximate depth of the ocean mixed layer, with the salinity difference shaded; and (c) a plot of potential temperature vs salinity, with isopycnals and the freezing point (dashed line) marked. The pressures of 125 and 300 db correspond to depths of 123.7 and 296.8 m, respectively.

~68°S, 70°W) but four days apart (9 and 13 October 2001, when the ship was "beset" by heavy ice conditions). The temperature and salinity (*T/S*) profiles in Fig. 8a clearly show a freshening of the ocean surface layer due to the widespread melt driven by the anomalous atmospheric circulation pattern. This occurred at a time when no significant change was observed in the upper-ocean temperature profile, that is, the mixed layer remained at freezing point (–1.8°C). Figure 8b is a close-up of the salinity profiles across the approximate depth of the mixed layer, with the salinity difference shaded. Figure 8c is a plot of potential temperature versus salinity illustrating the temporal change in salinity in the ocean mixed layer while the deeper waters remained virtually the same.

These data were used to calculate the magnitude of ice melt responsible for the observed ocean freshening, using the relationship

$$h_i = \Sigma[(S1_j - S2_j)/(S2_j - S_i)/\mathrm{WMLD}], \qquad (2)$$

where h_i is the ice thickness that has to be melted, S_i is the salinity of the ice to be melted (5 psu, based on analysis of the ice cores), $S1_j$ is the salinity of the first ocean profile at depth interval j, $S2_j$ is the salinity of the second profile at depth interval j, and WMLD is the winter mixed-layer depth (−125 db, corresponding to a depth of 123.7 m for the 9 October cast). As such, $\Sigma(S2_j - S_i)/\mathrm{WMLD}$ is the average salinity difference over the ocean mixed layer. In this case, $h_i = 0.08$ m of ice melt over the 4-day period, requiring, on average, ~70 Wm^{-2} of heating.

An assumption is made that the ocean freshening was due in this case to sea ice melt, rather than the horizontal under-ice advection of freshwater derived from glacier melt. However, the latter may be in evidence from longer profile comparisons, for example, comparing profiles from before 9 October, which showed the ship drifting over a front between 7 and 9 October. The profiles crossing the front show dramatic intrusions at the base of the mixed layer with considerable freshen-

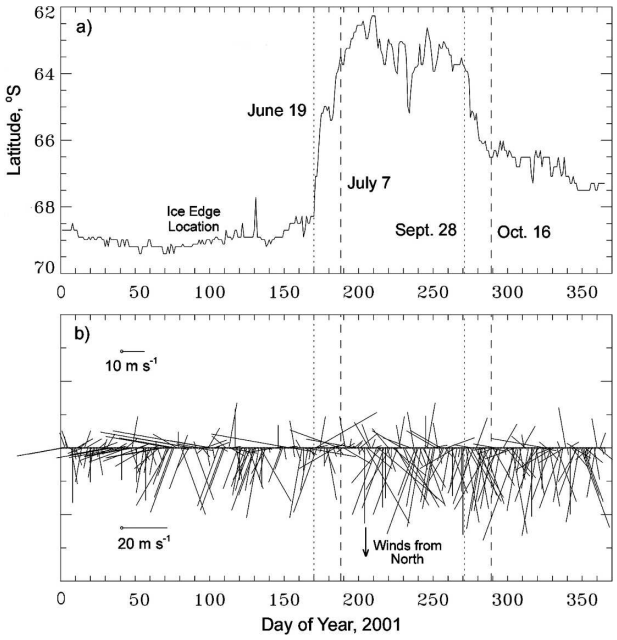

FIG. 9. (a) The daily advance and retreat of the sea ice edge location (15% ice concentration threshold) along the 70°W meridian. (b) Plot of daily (2400 UTC) wind speed and direction measured at Rothera Station (ID 89062; 67.51°S, 68.1°W). Periods marked by vertical dotted and dashed lines are discussed in the text.

ing (almost 0.40 m of ice melt if that is the source, and at this depth, we assume that it is from associated melting of glaciers in the region).

c. *Sea ice dynamics—Major compaction and anomalous ice extent*

The anomalous atmospheric circulation had an immense impact not only on sea ice thermodynamic but also dynamic processes, and once again over an extensive area. The net dynamic effect of the strong and persistent north-northwesterly winds was extreme compaction of ice into bays and against the western Antarctic Peninsula and adjacent islands. This created a heavily deformed and compact (high concentration) ice cover with a rough surface in the Bellingshausen Sea.

Figure 9a is a plot of the latitude of daily SSM/I-derived ice edge location (taken to be the 15% ice concentration threshold) along the 70°W meridian at daily intervals for 2001. For comparison, daily sea ice extent was also plotted within the LTER region and for the entire Bellingshausen region (60°–90°W), not shown here. A striking similarity in the patterns again highlights the regional impact of the atmospheric anomaly. Two 18-day periods have been bracketed—one during a time of accelerated advance (19 June to 7 July) and another during a time of accelerated retreat (28 September to 16 October). The latter coincides with the establishment (onset) of the atmospheric anomaly. Over the accelerated advance period, the ice edge moved equatorward by ~540 km along 70°W (from 68.28° to 63.44°S), equivalent to an advance of ~30 km per day (at an average speed of ~0.35 m s^{-1}). The accelerated retreat from 28 September to 16 October, on the other hand, moved the ice edge poleward by approximately 300 km along 70°W (from 63.8° to 66.51°S), or a retreat of ~17 km per day (at an average speed of ~0.20 m s^{-1}). Based on the meteorological data from the ship (as plotted in Fig. 5), the mean wind speed was 11.15 m s^{-1} and almost exclusively from the north. The strong northerly component is confirmed in daily wind speed and direction data collected at 2400 UTC at Rothera station, and plotted in Fig. 9b. If sea ice was drifting at ~2% of the wind speed, as postulated by Nansen's drift rule (Nansen 1902), then it would drift at ~0.22 m s^{-1}—similar to the average speed calculated above. The SSM/I data show that sea ice areal extent in the sector 60°–80°W decreased by fully ~43% (from ~0.62 to 0.36 × 10^6 km^2) over the period 1–14 October 2001, that is, immediately after the onset of the anomalous atmospheric circulation pattern.

The dominance of a southward drift pattern and the resultant highly convergent nature of the ice cover in the late austral winter to spring of 2001 is further illustrated by the drift behavior of a satellite-tracked Argos buoy (ID 7949) deployed on an ice floe in the mouth of Marguerite Bay in early August 2001 (see Fig. 10 of Perovich et al. 2004). After initially heading westward out of the bay then to the north-northeast, the buoy drifted virtually due south and covered only a relatively small distance. Dominant southward drift of buoy 7949 occurred approximately along the 72°W meridian toward the coast of Alexander Island from late September until late October 2001, when it deflected approximately southwestward before ceasing transmission on 10 November 2001 (Perovich et al. 2004). Heavy ice conditions, extreme convergence, and a lack of free drift account for the relatively short distance traveled by ice over this period—an impact also experienced by the R/V *Nathaniel B. Palmer*, which became beset only ~130 km from the open ocean. Under normal circumstances, the ice drift has a net northeastward component in the Bellingshausen Sea region, but with a much higher degree of variability at this time of year due to the passage of storms—although complex ocean surface current regimes occur within Marguerite Bay (Beardsley et al. 2004; Klinck et al. 2004). Monthly averaged ice motion maps derived from SSM/I data (not shown) fail to capture the southward ice drift very well but do illustrate a weak northward drift, implying southward ice

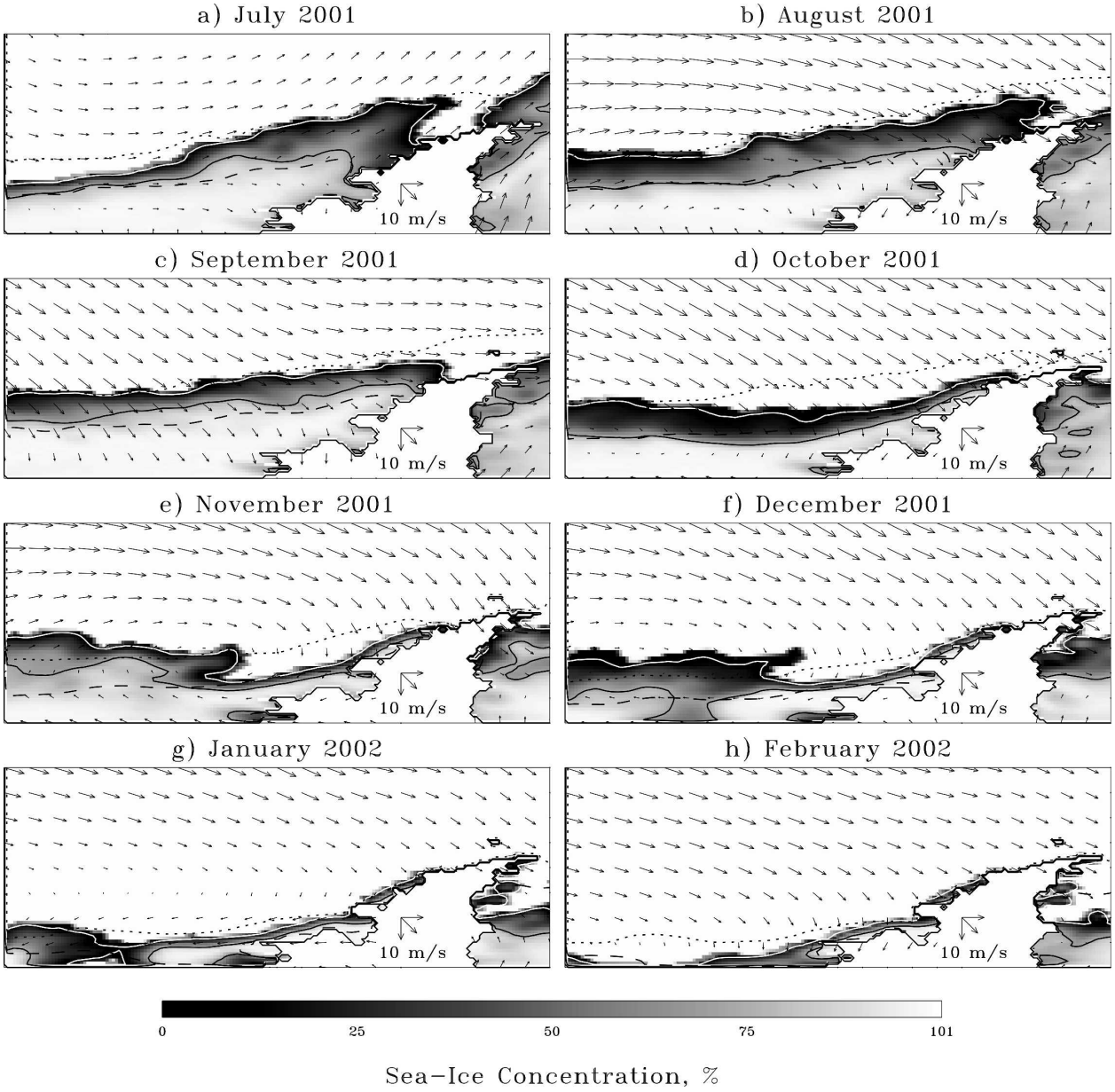

FIG. 10. Maps of monthly mean DMSP SSM/I sea ice concentrations in the WAP region from July 2001 to February 2002, with 15% and 75% ice concentration contours marked (the white and black lines, respectively). The long-term means (1980–2001) of the locations of the 15% and 75% ice concentration contours for each month are marked as black dotted and black dashed lines, respectively. Contemporary monthly mean wind velocity data from the NNR dataset are superimposed.

compaction and non-free-drift conditions in the spring–summer of 2001/02.

The dynamic processes outlined above also resulted in a highly anomalous seasonal sea ice areal extent in the austral spring through summer period of 2001/02 in the northwest Antarctic Peninsula sector. Compared to the long-term mean, sea ice extent was greatly reduced in October to December 2001, as shown in the sequence of SSM/I monthly average ice concentration and extent images in Fig. 10. The black dotted line in each represents the long-term mean ice edge location (taken to be the 15% ice concentration threshold) for that particular month over the period 1980–2001, derived from both SMMR and SSM/I data combined. The black dashed line is the 1980–2001 mean 75% ice concentration threshold and is included as a proxy indicator of the extent of the consolidated pack ice "core" region. Monthly mean wind velocities from the NNR dataset

are superimposed on the ice concentration/extent data in Fig. 10. The two datasets combined again clearly show the profound impact of the exceptional persistence of strong winds with a dominant north/northwesterly component over the West Antarctic Peninsula region over the period from October 2001 to February 2002 inclusive. This pattern is confirmed by Rothera meteorological data (see Fig. 9b). It is also apparent that the low ice extent persisted throughout October and beyond, coinciding with an increase in ice compactness (concentration). Taken together, these results indicate that the anomalous decrease in regional sea ice extent was predominantly driven by dynamic rather than thermodynamic processes. This is in line with similar findings from synoptic-scale studies of the region by Stammerjohn et al. (2003) and Harangozo (2004). Again, the extraordinary feature in 2001/02 is the duration of the impact.

The anomalously low seasonal extent in late 2001 coincided with an unusually short period of sea ice retreat for the region, as depicted in Fig. 9a. Generally, the period of ice retreat is relatively long (~7 months), compared to that of ice advance (~5 months; Stammerjohn and Smith 1996). Moreover, maximum ice extent in the WAP region occurred in June. This is atypically early compared to the average month of maximum sea ice extent for the WAP region (August; Gloersen et al. 1992), or compared to the late maximum in 2000 (September–November; Meredith et al. 2004). The unusual sea ice distribution in 2001/02 has implications for the ocean surface radiation budget and possibly changes in cyclone trajectories (Menendez et al. 1999; Murray and Simmonds 1995). Turner et al. (2003) report on a shorter-term (i.e., two-week) sea ice retreat that occurred in the Bellingshausen Sea in August (late winter) 1993.

The extreme ice compaction also gave rise to more extensive ice with above-normal ice concentrations near the coast throughout summer. As shown in Fig. 10, the overall areal extent was less than the 1980–2001 mean in January and February 2002, while the compact core for the same period, and marked by the 75% ice concentration contour, extended beyond the mean. Heavy ice conditions persisted not only in Marguerite Bay but also widely west of Alexander Island—in spite of the warm conditions and in a region where seasonal meltback normally occurs. An analysis of monthly mean passive-microwave-derived sea ice concentration maps showed that, over the period 1978–2002, sea ice persisted in summer throughout the Marguerite Bay region only in 2002, 1996, 1987–88, and 1978–84.

The exceptional atmospheric circulation pattern also produced unusual ice edge conditions. The circumpolar

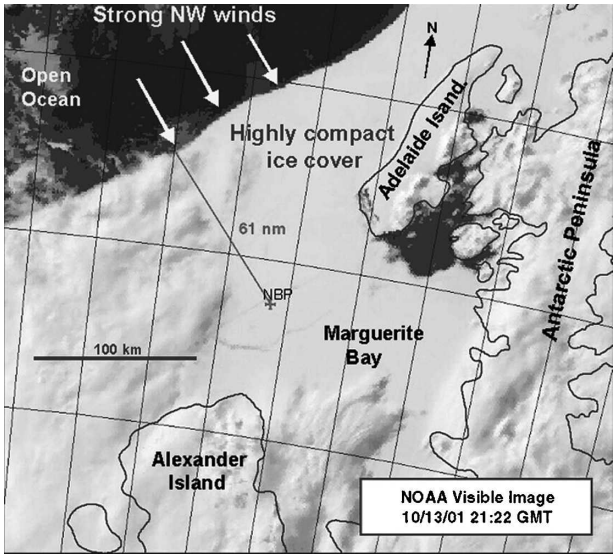

FIG. 11. NOAA AVHRR channel 1 (visible) image of the Marguerite Bay region, acquired at 2122 UTC on 13 Oct 2001, showing the extraordinarily compact and linear ice edge. Note the polynya on the downwind (lee) side of Adelaide Island. The ship's location is marked as NBP.

Antarctic marginal ice zone is typically highly diffuse and composed of series of ice edge bands rather than a distinct ice–ocean boundary, with periods of compaction being limited to periods of on-ice winds lasting a matter of days at any one time and related to the passage of storms. It can be seen from the NOAA AVHRR image in Fig. 11 that the situation was quite different in late 2001, however, with an extraordinarily compact marginal ice zone and linear ice edge over a broad section of the Bellingshausen Sea. The polynya adjacent to Adelaide Island is also noteworthy, insofar as it persisted in spite of the extreme ice compaction elsewhere in the region. These dominant features of the physical landscape will be further discussed in section 5 within the context of ecological impacts.

d. Immense dynamic sea ice thickening

The dominant ice convergence against the Peninsula and islands in response to persistent north-northwesterly winds led to immense dynamic thickening of the sea ice cover. This created an ice cover dominated by heavily ridged and rafted fragments of first-year ice, individually 0.5–1.5 m thick and stacked together to form a very thick stratum. Exceptional ice thicknesses resulted, presumably over a large area given that the ice edge retreat monitored in satellite data was so widespread (see Fig. 10). Indeed, scuba divers on the cruise estimated ice thicknesses in mid–Marguerite Bay of 10–15 m on 3 October, and even ~20 m on 13 October (see

TABLE 2. Mean ice thickness ($\overline{Z}_i$) and snow thickness ($\overline{Z}_S$) measured on other cruises to West Antarctica, and reported in the literature. ABS is the Amundsen–Bellingshausen Seas, and WRS is the western Ross Sea.

Distance from ice edge (km)	$\overline{Z}_i$ (m)	$\overline{Z}_S$ (m)	Date	Region	Reference
50–100	0.34	0.07	Aug–Sep 1993	ABS	Worby et al. (1996)
0–200	0.55 ± 0.24	0.07 ± 0.06	May–Jun 1995	WRS	Jeffries and Adolphs (1997)
0–200	0.22 ± 0.11	0.04 ± 0.03	Jun–Jul 1999	WAP	Smith and Stammerjohn (2001)
350–550	0.55	0.23	Aug–Sep 1993	ABS	Worby et al. (1996)
200–600	0.80 ± 0.38	0.17 ± 0.11	May–Jun 1995	WRS	Jeffries and Adolphs (1997)
200–550	0.49 ± 0.11	0.04 ± 0.03	Jun–Jul 1999	WAP	Smith and Stammerjohn (2001)
Avg	—	0.23 ± 0.16	Aug–Sep 1993	ABS	Jeffries et al. (1994b)
Avg	0.48	0.19	Aug–Sep 1993	ABS	Worby et al. (1996)
Avg	0.51 ± 0.27	0.11 ± 0.10	May–Jun 1995	WRS	Jeffries and Adolphs (1997)
Avg	0.36 ± 0.18	0.04 ± 0.03	Jun–Jul 1999	WAP	Smith and Stammerjohn (2001)

Fig. SM3). For comparison, mean ice (and snow) thicknesses measured on other cruises to the approximate region in different years are significantly lower, at <1 m (Table 2). For Antarctica as a whole, the usually divergent sea ice results in a seasonal cover that is more typically of the order of ~0.5 to 2 m in mean thickness (Worby et al. 1996). Contemporary ship observations of ice thickness during NBP01–05, and using the standard protocol of Worby and Allison (1999), seriously underestimated the actual thickness at this time. They yielded estimates of only 1–3 m (e.g., on 3 October), being based on observations of upper rafted blocks only, which were dislodged and overturned by the ship's hull. This was also the case with standard drill hole and ice core measurements, as these typically failed to penetrate the entire ice profile and therefore sample the upper horizons only, that is, a few rafted blocks, separated by interstitial water gaps of some tens of centimeters. As a result of these difficulties, it was impossible to measure the mean regional sea ice thickness in late 2001.

The rafted floes making up the very deep ice were largely frozen together (albeit with interstitial gaps), in spite of the warm temperatures in the surface air and through the ice column. It is thought that "cementing together" of stacked floes in this fashion under melt conditions occurred by the rapid refreezing of meltwater percolating downward through the porous sea ice matrix, as described in sections 4a and 4b. This low-salinity water would refreeze at a higher temperature than seawater at a salinity of ~35 psu. Unfortunately, deep ice core data were not collected to test this hypothesis, which is based on upper-core analysis and visual observations by the dive team. This scenario implies that the ice mass would not relax and disperse (i.e., thin with a collapse of rafted blocks), with a subsequent release of lateral ice pressure (change from convergent to divergent conditions)—to help perpetuate the ice through summer.

Substantial dynamic thickening was observed to occur during individual "cataclysmic" events, when the ice periodically "gave" mechanically in response to the immense pressure exerted by almost constant convergence against the Peninsula and islands over a number of days. One such event took place on 8 October. Over a matter of an hour or so, the relatively flat floe comprising an ice station was transformed to a jumbled mass of ice rubble by the severe mechanical pressure buildup within the ice cover. As a result of the extreme forces, ice was even rafted onto the back deck of the ship. This "icequake" coincided with winds of 15–20 m s^{-1} from the north (330°–30° T) and air temperatures of ~0.0° to –1.0°C, that is, typical conditions at this time.

The extreme compaction, thickness, and consolidation of the ice would help to explain the persistence of unusually heavy sea ice conditions throughout the austral summer. The lack of open water (leads) within the pack in spring–summer of 2001/02 would greatly diminish the normal seasonal ice decay process involving the absorption of incoming shortwave radiation by the ocean and associated lateral ice-floe melt (Perovich et al. 2003; Watkins and Simmonds 1999). Moreover, the extreme ice thickness would reduce the ability of vertical melt processes to completely remove the ice cover over the annual melt season in 2001/02. Other likely contributing factors related to the atmospheric anomaly include the greater-than-average snow accumulation, both observed and modeled (see below). This would also reduce the penetration/transmission of incident shortwave radiation into the underlying ice mass for melting (Eicken et al. 1995; Perovich 1996), given the

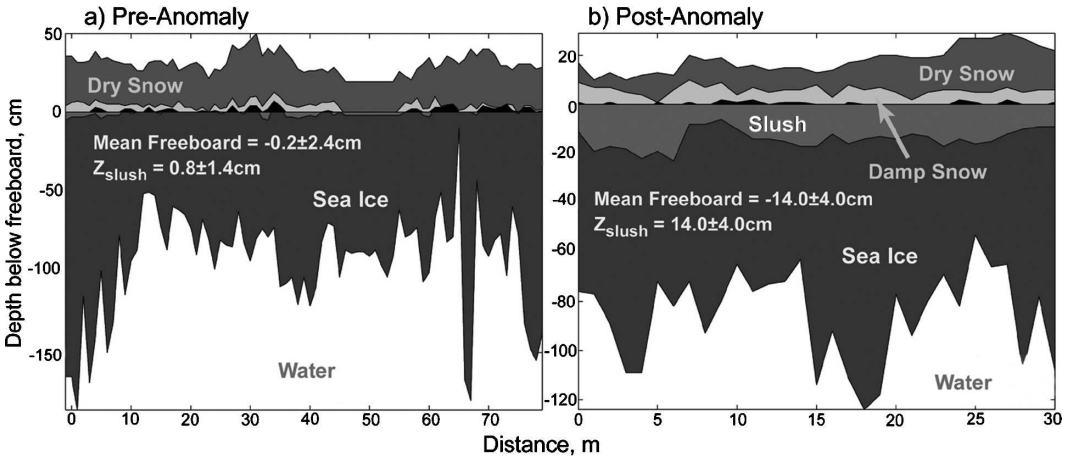

FIG. 12. Snow and ice thickness transects across two floes: (a) at ~67.5°S, 70.7°W on 16–17 Sep 2001 (prior to the onset of the atmospheric circulation anomaly) and (b) at 68.25°S, 69.8°W on 30 Sep (after the anomaly onset), where 0 cm is sea level. Thickness profiles of the flooded layer, damp, and saturated snow are also marked.

high optical extinction coefficient of snow (Warren 1982). Snow also has excellent insulative properties (Massom et al. 2001).

e. Elevated snow cover thickness, surface flooding, and snow-ice formation

The anomalous atmospheric circulation pattern in 2001/02 advected more moisture over the Bellingshausen Sea ice zone than normal, leading to anomalously high precipitation rates over an extended period. Time series of monthly mean precipitation rates derived from NNR data at 65°S, 70°W, and shown in Fig. 7e, indicate that although high snowfalls occurred at other times (e.g., in 1994 and 2000), they were at no time as protracted as in late 2001. Prolonged storminess and frequent snowfalls under blizzard conditions led to significant wind redistribution and an average snow cover thickness (Z_s) in September–October 2001 of ~0.37 m (standard deviation = ~0.13 m, n = 286) over the highly deformed first-year sea ice (determined from in situ thickness transects at 0.5–1.0-m intervals). This is significantly higher than previous observations in the approximate region and during the austral winter–spring, for example, Jeffries et al. (1994b) reported a mean Z_s of 0.23 m for the sector 75°–110°W for 1993. Elevated localized snow accumulation occurred because of the rough nature of the ice surface, with significant dune and sastrugi formation adjacent to ridge sails and other surface roughness features [in the manner described by Massom et al. (2001)]. Mean snow thickness values reported from other previous cruises to the region are given in Table 2 for comparison. The occurrence of a heavy snowfall in the spring of 2001 is confirmed by data collected by an autonomous mass balance buoy deployed in Marguerite Bay in August (Perovich et al. 2004). In this case, the snow depth increased by >1 m between 6 August and 6 November of 2001.

Widespread flooding of the snow–ice interface was a defining feature, as shown in Fig. SM4. The resultant increase in ice surface flooding as the anomalous atmospheric circulation pattern developed in September is shown in Fig. 12. This presents snow and ice thickness (drill hole) transects across two large and relatively flat first-year floes from roughly the same region taken about a week prior to the onset of the anomalous atmospheric circulation pattern (Fig. 12a), and a few days after it (Fig. 12b). An increase in flooding is also apparent in Table 3, which presents mean values from these transects (plus an intervening transect). Based upon 235 measurements along transects across floes, the mean freeboard overall was –6.4 cm (standard deviation = 14.7 cm). This compares to average freeboards reported in the region by Perovich et al. (2004) of –1 and +5 cm in July–August of 2001 and August–early September of 2002, respectively. In viewing the above table and Fig. 12b, it is important to recall that the ice thickness Z_{ice} measured in late September–October represents only that portion of the total overrafted ice thickness that could be sampled from the surface, that is, typically only the upper few meters.

Surface flooding of Antarctic sea ice within inner pack regions is in general largely associated with the snow-loading effect, whereby the ratio of snow to ice thickness tends to be large enough to affect floe isostasy and depress the ice surface below sea level (Eicken et al. 1995; Jeffries et al. 1998; Lange et al. 1990; Massom et al. 2001). That flooding took place over such an ex-

TABLE 3. Mean values of the thicknesses of snow (Z_s), ice (Z_{ice}), freeboard, slush layer (Z_{slush}), and wicked layer (Z_{wicked}), freeboard, and ice surface temperature (T_{is}) along three transects. Transect 2 was at ~68.0°S, 69.9°W. Units are centimeters. Zero freeboard is sea level, and negative values indicate below sea level.

Transect	Z_s	Z_{ice}	Freeboard (cm)	Z_{slush}	Z_{wicked}	T_{is}
TR1, 16–17 Sep $n = 80$	30.2 ± 6.5	93.6 ± 33.0	−0.2 ± 2.4	0.8 ± 1.4	4.1 ± 3.2	−2.1 ± 0.4
TR2, 26 Sep $n = 50$	51.6 ± 9.0	89.9 ± 32.8	−16.3 ± 7.6	18.3 ± 5.2	25.0 ± 6.2	−1.8 ± 0.1
TR3, 30 Sep $n = 30$	32.1 ± 4.9	71.4 ± 19.1	−14.0 ± 4.1	14.0 ± 4.0	19.0 ± 4.0	−1.9 ± 0.1

tremely thick ice cover in October 2001 is due to a number of factors. Although the total ice thickness was substantial, the ice mass comprised a series of rafted first-year floes, stacked on top of each other and individually separated by interstitial seawater-filled gaps. Key factors at this time, and in addition to elevated snowfall, were the extreme ice deformation and warm conditions (the latter enhanced and perpetuated by the snow cover). Deformation would act to depress a significant proportion of the ice surface below sea level, with seawater then flooding the surface by lateral intrusion from floe edges. The consistently high temperatures played an important role by increasing the porosity/permeability of the ice, as discussed in section 4a (see also Perovich et al. 2004). This in turn facilitated the upward incursion of seawater onto the ice surface through enlarged and interconnected brine channels, in the manner described by Golden et al. (1998).

Typical surface conditions encountered under the high-temperature regime included a thick layer of slush overlying the sea ice proper, with a large negative (up to –0.35 m) freeboard (see Fig. SM4a). The high-salinity freezing slush layer comprised up to more than half of the total snow column from the ice surface upward, followed by a layer of wicked damp and saturated snow with a mean salinity of ~5 psu. This was typically capped by a layer of relatively dry snow with a low salinity (i.e., <1 psu). The elevated salinity and wetness of the snow likely had a significant effect on both the optical and microwave properties of the ice, with implications for the sea ice biota, the surface energy balance, and the interpretation of satellite data. Snow salinity also changes its freezing/melting point.

Although temporary, periodic decreases in air temperature shown in Fig. 5 were of sufficient magnitude and duration to freeze the slush, leading to substantial snow–ice formation. The resultant increase in the occurrence of snow–ice (the meteoric component) after the onset of the anomalous atmospheric circulation pattern is borne out by $\delta^{18}O$ analysis of ice core samples collected during the cruise and shown in Fig. 13. In this figure, profiles of ice $\delta^{18}O$ as a function of depth below the ice surface are split into three 10-day segments to highlight the impact of the anomaly. The first plot combines all ice core data from 16–26 September, corresponding to the period immediately prior to the anomaly onset, while the second plot spans the onset and a few days beyond and the third plot (8–18 October) illustrates data from after the establishment of the anomalous pattern. Again following Jeffries et al. (1998) and Eicken (1998), snow–ice, that is, ice with a meteoric component rather than exclusively frozen seawater, is defined as granular ice with a $\delta^{18}O$ value of <0. The peak in the incidence of snow–ice below ~1 m in the ice column corresponds to the downward movement of a floe surface by rafting, and/or the refreezing of downward-percolating snow meltwater in the form of dendrites on the base of rafted blocks (see section 4a). This transformation of conditions from September to October 2001 would help to explain the apparent thinning of the "dry" snow cover over time in Fig. 12, with an increasing proportion of the vertical snow column being incorporated into slush and snow–ice formation. Taken overall, these findings are in line with recent observational and modeling studies, for example, Fichefet and Morales Maqueda (1999), Perovich et al. (2004), and Wu et al. (1999), which show that snow–ice plays a major role in the seasonal growth and decay cycles of Antarctic sea ice. In this case, the impact is profound and complex.

5. Ecological impacts

As stated above, the structure and function of all levels of the Antarctic marine ecosystem are intimately coupled to the annual advance, retreat, and intervening behavior and characteristics of the sea ice cover (Smith et al. 1995; Ross et al. 1996). Because of its magnitude and persistence, the anomalous atmospheric circulation impacting the West Antarctic Peninsula sea ice habitat in 2001/02 was complex and profound, and arguably both positive and negative. The impacts of the anomalous atmospheric and sea ice conditions on the sea ice

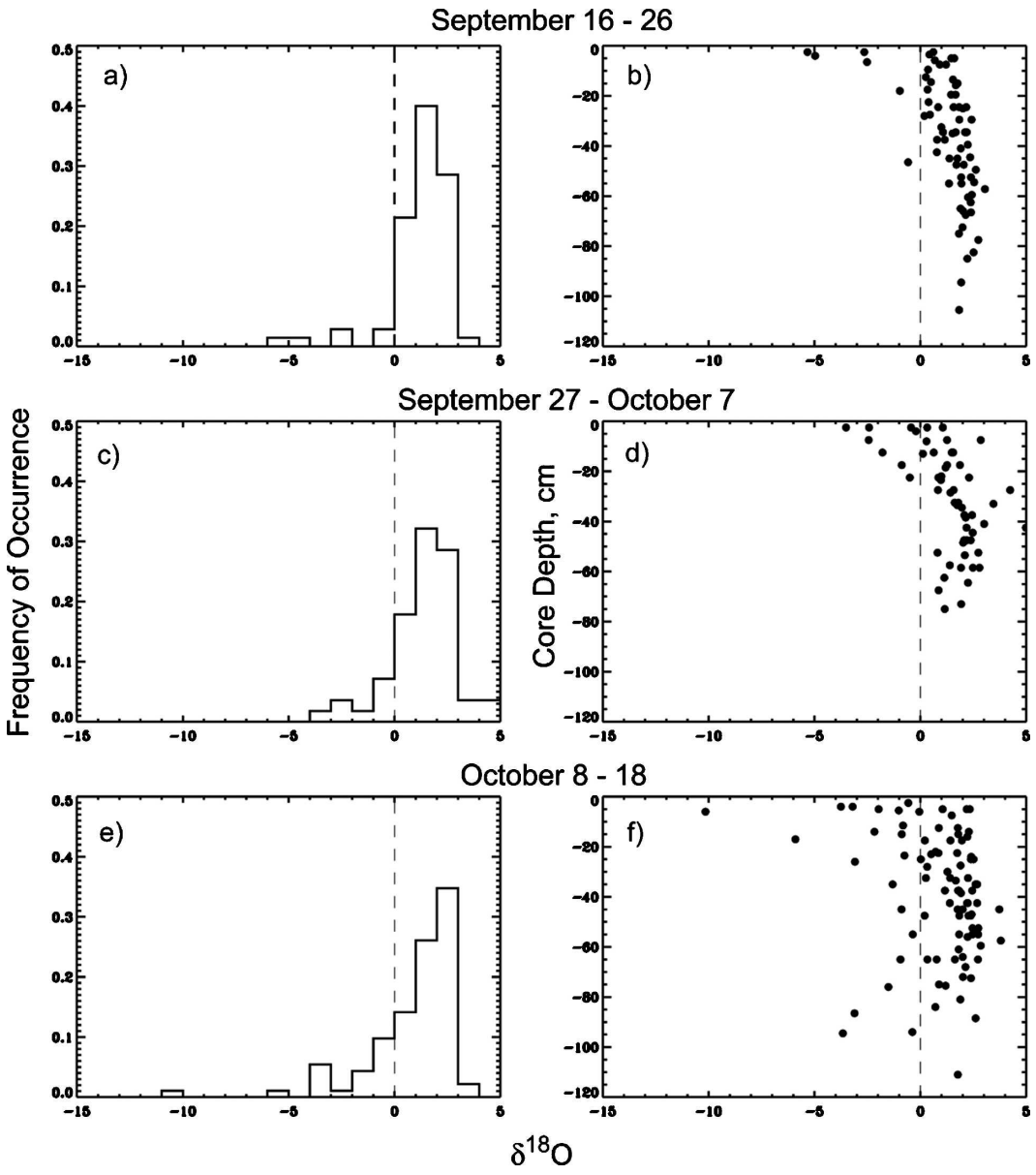

FIG. 13. Paired plots of the frequency distributions of $\delta^{18}O$ values of ice cores and $\delta^{18}O$ as a function of depth in the ice core below the icefloe surface, over three 10-day periods: (a), (b) 16–26 Sep; (c), (d) 27 Sep–7 Oct; and (e), (f) 8–18 Oct 2001.

ecosystem continued throughout the spring–summer period and possibly beyond.

a. Positive impacts

At the lower trophic level, the widespread flooding of the snow–ice interface had a major impact on regional primary production by bringing phytoplankton and nutrients to the ice surface, where they concentrated to form a thriving "infiltration" community. These observations support the results of Arrigo et al. (1997) and Fritsen et al. (1998). The latter found that increased flooding in regions with thick snow cover [and in this case extreme ice deformation and persistently warm (porous) ice] enhances primary production in the infiltration (surface) layer, and that productivity in the freeboard (sea level) layer is also determined by sea ice porosity, which varies with temperature (Golden et al. 1998). Elevated primary production of sea ice phytoplankton resulted, in response to higher levels of photosynthetically available radiation (PAR) at the ice surface compared to depth (Horner et al.

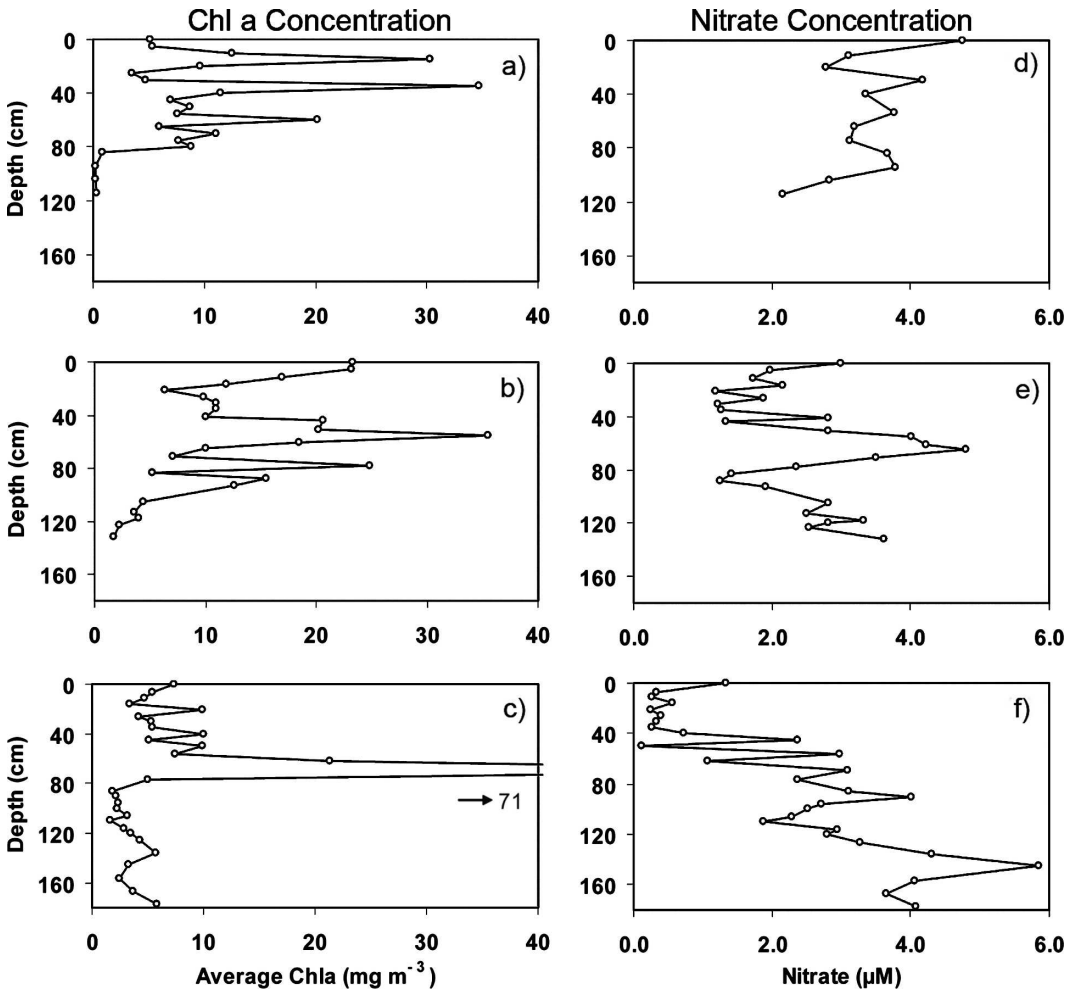

FIG. 14. Profiles of (a)–(c) ice algal biomass as chlorophyll *a* in mg m^{-3} and (d)–(f) nutrients as nitrate in μM for three time intervals during the study period: (a), (d) 16–26 September, (b), (e) 27 September–7 October, and (c), (f) 7–17 October. For the first period, averages for three cores are presented, sampled at 5-cm intervals (20 depths), where $n = 44$. During the second period, six cores were sampled at a 5-cm resolution and 23 depth intervals, with $n = 82$. During the third period, five cores were sampled at 5-cm intervals, at 28 different depths, $n = 91$.

1992). This resulted in a significant contrast between the ocean and ice, with phytoplankton biomass and primary production in the water column being consistently low compared to levels in the ice.

Algal biomass within the ice, measured as chlorophyll *a* (chl-*a*), showed a vertical distribution characterized by several layers of high concentration. These layers exhibited a high degree of discoloration to the naked eye (see Fig. SM4b). Biomass concentration was 3–9 times greater in the layers compared to the background concentration. As shown in Fig. 14, the layers averaged 28.3, 21.1, and 47.7 mg chl-*a* m^{-3} within a background of 4.7, 6.4, and 4.7 mg chl-*a* m^{-3} for the three time periods analyzed. These correspond to the periods in Fig. 13, that is, prior to, during, and after the establishment of the anomalous atmospheric circulation pattern. The distinct layers in Fig. 14 were probably formed by the burial of individual infiltration communities by the extensive over-rafting of floes. This is supported by the distance between individual layers, which approximately corresponds to the thickness of individual first-year floes making up the rafted thick ice, as determined from the in situ drilling program.

A marked temporal progression was observed in biomass distribution within the ice, coinciding with the observed increase in ice compaction and thickness and the change in ice conditions described above. Chlorophyll *a* (chl-*a*) was found throughout the upper ice column (note again that only the upper ice column was sampled), independent of ice thickness and throughout

TABLE 4. Chlorophyll *a* concentrations (in mg m^{-3}) and nutrient concentrations (in μM) in the ice column sampled and averaged in the three 10-day periods from mid-September to mid-October 2001. In these periods, $n = 44$, $n = 82$, and $n = 91$, respectively.

Period	Chl *a*	Phosphate	Silica	Nitrate	Ammonium
16–26 Sep	9.59 ± 9.25	0.33 ± 0.99	9.53 ± 1.84	3.38 ± 0.69	1.67 ± 1.79
27 Sep–7 Oct	12.9 ± 8.6	0.37 ± 0.14	9.1 ± 2.9	2.48 ± 1.04	0.53 ± 0.22
8–18 Oct	7.7 ± 13.1	0.35 ± 0.19	10.76 ± 4.6	2.2 ± 1.55	0.75 ± 0.41

the sampling period (Fig. 14). The average number of layers of high chl-*a* concentration, however, decreased from September to October 2001, that is, from 3 to 1. Second, the total integrated chl-*a* showed a maximum at the beginning of October 2001. Integrated chl-*a* values for the three 10-day periods depicted in Fig. 14 are 195.5, 309.5, and 222.1 mg chl-*a* m^{-2}, respectively. By comparison, average values of chl-*a* in the top few meters of the water column were (i) 16–26 September: 0.13 ± 0.08 mg chl-*a* m^{-2} ($n = 8$); (ii) 27 September to 7 October: 0.09 ± 0.04 mg chl-*a* m^{-2} ($n = 4$); and (iii) 8 to 18 October: 0.15 ± 0.08 mg chl-*a* m^{-2} ($n = 4$).

Unlike chl-*a*, macronutrient concentration (nitrate, nitrite, silicic acid, and orthophosphate) showed a less widely varying distribution with depth in the ice (Fig. 14). The overall concentration was lower than in the water column, for example, the average concentration of nitrate was 2.5 μM in the ice versus 28 μM in the upper water column. Some layering was also observed, but this was not as pronounced as for the chl-*a* distribution. In the case of nitrate, there is a suggestion that the nutrient layers could originate from biological activity, as local minima coincide with chl-*a* maxima.

Results presented in Table 4 show that all of the analyses varied with time. Average nutrient concentration did not change with time, however. Vertical distributions in the ice column changed dramatically from a fairly uniform distribution in mid-September to low concentrations at the surface a month later. By mid-October, nitrate concentration became apparently limiting in the upper 0.5 m of the ice column (0.2 μM). High ice porosity and homogeneous temperature profiles in the ice column suggest that flooding of seawater at the snow–ice interface was initially the source of nutrients to the ice communities. This scenario is consistent with the homogeneous nutrient distribution found in mid-September. By mid-October, the increase in ice convergence and the extensive over-rafting of ice floes could explain the marked increase in nutrient concentration with depth, although the exact mechanism required to maintain such a distribution is not apparent from the data. Another factor could again be the elevated surface melt, with gravitational downward percolation of meltwater through enlarged brine-drainage channels flushing nutrients down through the ice column. The increase in ice porosity with temperature could have a double-edged effect, both by allowing (i) the upward percolation of seawater through the ice column to flood the surface and (ii) the downward movement of meltwater. Further work is necessary to examine these processes and their biological role on the microscale.

The high ice biomass observed during this cruise is believed to relate to the particular sea ice dynamics encountered in 2001. While there are few measurements of chl-*a* in sea ice in the WAP region for comparison, available data exhibit great variability in austral autumn/winter concentrations. Chlorophyll *a* concentrations averaged 0.55 mg m^{-3} during June–July 1999, with coincident water column chlorophyll-*a* concentrations that were again relatively low (0.03–0.05 mg m^{-3}) throughout the sampling area during this early winter period (R. C. Smith 2005, unpublished manuscript). In May–June 2001, chl-*a* concentrations in newly formed pancake ice were high, with an average of 13.8 mg m^{-3} where n = 2 (M. Vernet 2005, unpublished manuscript). These results suggest that the high chl-*a* concentrations found in September and October 2001 were due to a combination of factors, from high chl-*a* entrainment during formation in late austral autumn to a persistent late spring sea ice, described in this study (see also R. C. Smith et al. 2006, unpublished manuscript).

A MAJOR PHYTOPLANKTON BLOOM BOTH WITHIN AND OUTSIDE THE ICE EDGE

The exceptional conditions in late 2001 also contributed to major phytoplankton bloom conditions in the WAP. Enhanced ice deformation, snowfall, and flooding in September–October 2001 resulted in the incorporation of a major "reservoir" of biological material into the sea ice (as described above). On traversing the marginal ice zone on 22 October (at ~64.75°S, 64.90°W), the ship encountered an unusual phytoplankton bloom poleward of the sea ice edge, and within a 100% ice cover. Wave–ice interaction was a key physical and biological process, with a 2–3-m swell from the northwest leading to snow cover removal and surface wetting by wave overwashing and floe–floe buffeting, the latter process introducing additional algae onto the

ice surface. It also compacted the marginal ice zone (see Fig. 11) and induced floe–floe pulverization. These processes mechanically broke down the sea ice to release the phytoplankton contained within it. This created an unconsolidated 100% cover of brash-ice fragments (up to 1–3 m in diameter) separated by an interstitial dark-green slurry of frazil ice/slush and biological material combined, which was constantly reworked by the swell (see Fig. SM5). In this manner, sea ice algae were exposed to significantly higher levels of PAR and macronutrients, compared to a consolidated ice cover with a snow cover. The net effect was the creation of an "intrapack" bloom relatively far to the south and unusually early in the season.

The intensity of this bloom, which extended across a zone some tens of kilometers wide, is indicated by the darkness of the green discoloration of the combined frazil–phytoplankton slurry. This significant decrease in surface albedo, again compared to that of consolidated pack with a snow cover, would lead to a positive feedback effect, whereby enhanced absorption of shortwave radiation as spring progressed would combine with the warm air being advected across the region to enhance melt of the slurry and phytoplankton release into the underlying water column. Stratification of the ocean mixed layer due to meltwater input over an extended period, both by ice melt and snow removal by wave overwashing, likely also contributed to the bloom conditions.

This "biological soup" resulted in a high degree of foraging activity at higher trophic levels. High concentrations of Adélie penguins (*Pygoscelis adeliae*) were observed inside the ice edge, typically in groups of 10–20, as well as crabeater seals (*Lobodon carcinophagus*), hunting leopard seals (*Hydrurga leptonyx*), and killer whales (*Orcinus orca*). Concentrations of Chinstrap penguins (*Pygoscelis antarctica*), Snow Petrels (*Pagrodama nivea*, one group consisted of over 40 individuals), Antarctic Petrels (*Thalassoica antarctica*), and Antarctic Terns (*Sterna vittata*) occurred at and just seaward of the ice edge proper. Previous studies (e.g., Smith and Nelson 1985) have reported on the occurrence of open-ocean blooms associated with the ice edge retreat, where there is an increase in water column stability due to meltwater input coupled with the release of algae "trapped" in the ice. What is unusual about the bloom encountered in October 2001 is that it initially occurred relatively early in the season, within the sea ice zone itself (in the presence of a 100% ice cover) and over a zone some tens of kilometers wide. Unfortunately, no direct measurements were made of this biological soup.

The intensity of the bloom, and its extensive coverage, is illustrated by analysis of satellite ocean color data derived from SeaWiFS. The data used are from the climatology of R. C. Smith et al. (2006, unpublished manuscript), comprising seven seasons of SeaWiFS data (1997/98 through 2003/04) for an extended region west of the Antarctic Peninsula. Monthly averaged Global Area Coverage (GAC) SeaWiFS data for this extended grid were themselves averaged to compute a chl-*a* climatology for each month for which the solar elevation and sea ice coverage permit adequate ocean color data to be obtained, that is, September through April. The impact of cloud cover was minimized by the averaging process. Anomaly maps for each of the seven seasons, and each month, were then computed as the difference between the monthly average data and the mean climatology. The current paper uses a small subset of this dataset, that is, from October 2001 through January 2002 inclusive, to illustrate the extraordinary nature of conditions in the austral spring–summer of 2001/02.

Results are given in Fig. 15 and show that the months following the establishment of the atmospheric anomaly exhibited significant ocean color anomalies in the WAP region. Of immediate note is an apparent stark contrast between phytoplankton distributions in October compared to November through January. In spite of the fact that the extensive intra-ice bloom occurred in October 2001, this month is characterized by an anomalously low pigment biomass seaward of the compacted ice edge (see Fig. 15e). Indeed, this was the lowest October value for the seven seasons of SeaWiFS data under study. These low values are attributed to the persistence of anomalously very strong north-northwest winds, which continued to pack the sea ice against the peninsula and created a deep ocean mixed layer unsuitable for bloom conditions. Note, however, that the open-ocean negative biomass anomaly occurred at the same time, that is, October 2001, as the extensive bloom within the sea ice zone itself. An important point here is that the latter could not be detected in SeaWiFS data. Average wind strength diminished in November, and, with the increasing solar radiation, a strong bloom appeared over the shelf and along the shelf break throughout the region as the ice edge receded. The phytoplankton bloom continued in the WAP area through the following months and produced the highest November and December chlorophyll anomalies for the seven seasons from 1997/98 through 2003/04. It is hypothesized that the compacted and over-rafted sea ice contributed melt water stability, nutrients, and a copious phytoplankton seed population that gave rise to the anomalously high late-spring and early-summer bloom, that is, the latter was conditioned by the anoma-

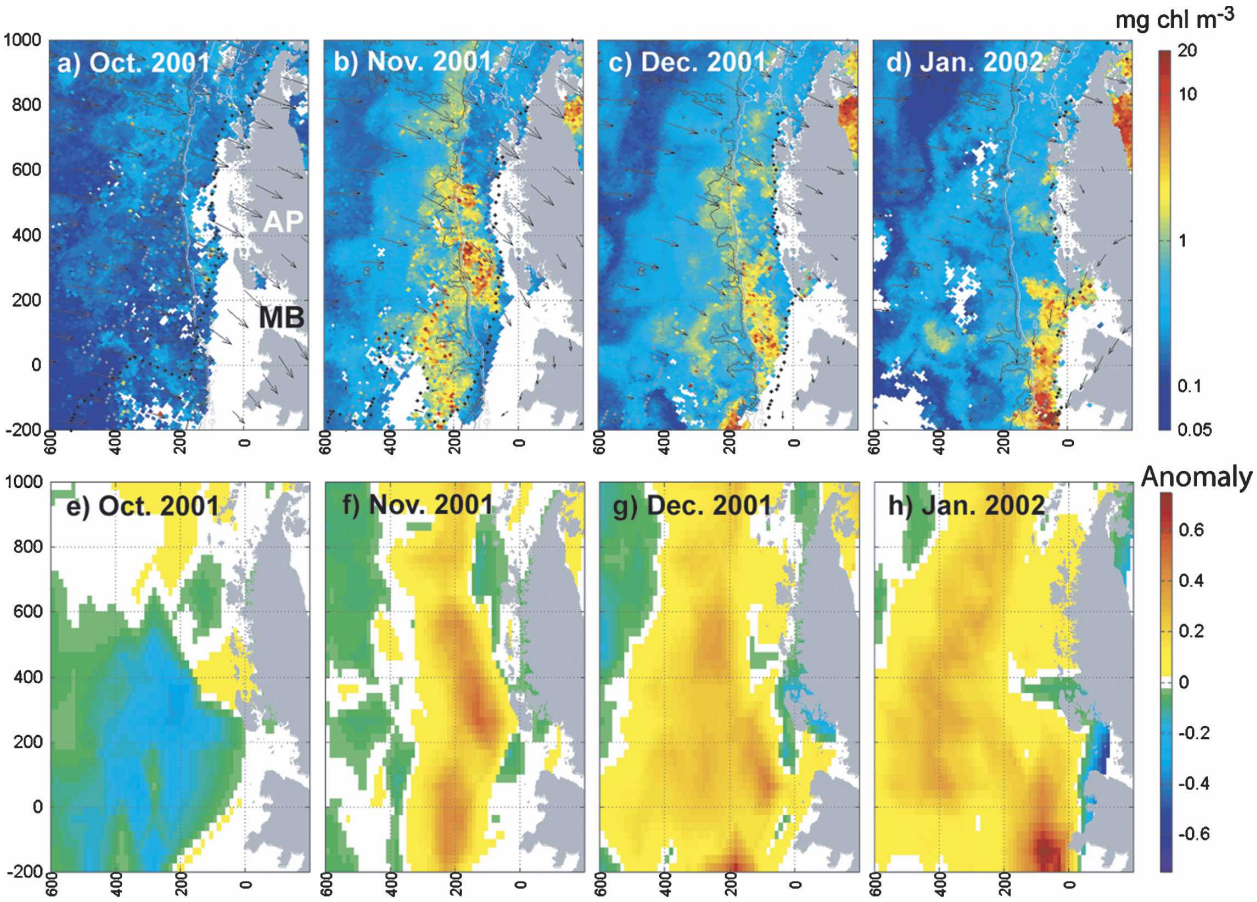

FIG. 15. Monthly averaged GAC SeaWiFS images of the WAP region for the period October 2001–January 2002 showing (a)–(d) pigment biomass and (e)–(h) monthly anomalies of pigment biomass, computed as the difference between the actual month and the 7-yr SeaWiFS climatology (not shown here). In (a)–(d), the following are marked: 500- and 1000-m ocean depth contours (white and black lines, respectively), sea ice extent at the beginning and end of each month (dotted gray and black lines, respectively), and monthly averaged NNR project wind speed vectors (black arrows). Sea ice is masked in white. AP is the Antarctic Peninsula and MB is Marguerite Bay. Dimensions are in kilometers.

lous atmospheric circulation. Note again that the bloom was detected in SeaWiFS data only when the ice edge receded, that is, in open-ocean conditions.

b. Complex impact on krill

Antarctic krill (*Euphausia superba*) are a major element of the Antarctic marine ecosystem and are closely coupled to sea ice at various key stages of their life cycle (Quetin and Ross 1991, 2001, 2003). Anomalous extreme ice conditions, such as those observed in late 2001 to early 2002, are likely to affect the under-ice habitat, which larval krill use as a source of food in winter and spring when food in the water column is scarce. Although scuba diving in late 2001 was limited by the heavy ice conditions, an abundance of larval krill was observed during the dives within the gaps and crevices created by rafted ice blocks, and extending to greater depths than observed during previous winter cruises to the west of the Antarctic Peninsula (Quetin et al. 1996; Frazer et al. 1997).

Although the larval krill were observed feeding on the floors, sides and "caves" formed by the over-rafted pack ice, one question concerned whether larval krill were able to find sufficient food to grow since primary production would normally be low at high latitudes within a 20-m thick ice column. In situ growth experiments with larval krill, as described in detail in Quetin et al. (2003) and Ross et al. (2004), yielded anomalous results compared to previous cruises. During two previous cruises in the September–October time period in WAP waters, growth increments in larval krill were positive and relatively high, ranging from 7% to 13% per intermolt period (Quetin et al. 2003). In September/October of 2001, however, the growth increments were negative, showing that larval krill were shrinking rather

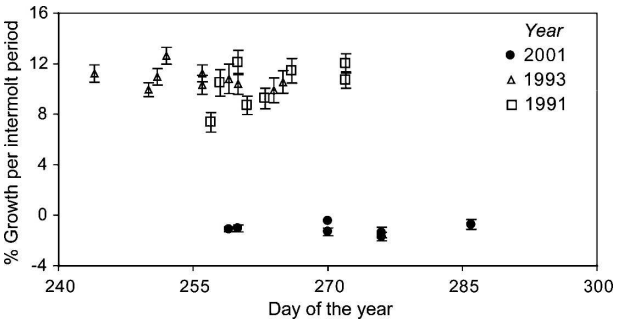

FIG. 16. In situ growth increments (% growth per intermolt period) for larval Antarctic krill collected from under the ice in austral spring of 1991 (open squares), 1993 (open triangles), and 2001 (closed circles). Larvae collected in 2001 averaged from 9.6 to 11.1 mm in total length. Points are the mean growth increment for an experiment with from 7 to 15 individual measurements. Error bars are standard error.

than growing (Fig. 16). The median intermolt period was 31 days. The following January, the young-of-the-year caught during the Palmer LTER annual cruise were still abundant, but were found in two modes with mean total lengths of 16.75 and 25.35 mm, respectively (Quetin and Ross 2003). The mode of smaller young-of-the-year might be derived from a late second spawning or from that part of the larval population living in the deeply over-rafted pack ice where growth rates remained negative late into the austral spring.

Previous work has shown that interstitial cavities between ice-rafted blocks play an important role in the larval-stage ecology of krill (Frazer et al. 1997; Ross et al. 2004). The likely benefits of rafting gaps to krill result from the fact that they form (i) a relatively quiescent and stable environment, enabling krill to drift with the ice with minimal energy expenditure; (ii) protection from large predators; and (iii) a concentrated food source relative to the underlying water column. Having said this, and in spite of the apparent downward injection of phytoplankton biomass by the rafting process (section 5a and Fig. 14), it appears that insufficient food was available under the extreme ice conditions in 2001/02 to engender the growth of larval krill inhabiting the ice cavities. Clearly, more work is necessary to better understand krill ecology relative to such habitat complexity.

c. *Negative impacts*

The circumstances associated with the unprecedented atmospheric circulation in the WAP region from late austral winter through spring to summer of 2001/02 had adverse effects not only on krill but also on apex predators, such as Adélie penguins (*Pygoscelis adeliae*). Annual changes in the populations of this species occur in response to two scales of processes. At regional scales, the presence or absence of sea ice determines the number of breeders that annually attempt to reproduce, while at local scales, variability in snow accumulation affects seasonal reproductive success (Fraser et al. 1992; Fraser and Patterson 1997; Patterson et al. 2003). Over ecological time (decades to centuries), the combined effects of these and other processes determine to what extent habitat conditions are optimal for Adélie penguins, and, ultimately, local to regional long-term population trends (Fraser and Trivelpiece 1996).

The unique environmental situation apparent during 2001/02 provided an unusual opportunity to observe how interactions between adverse sea ice conditions and high snow accumulations affected Adélie penguins in the Palmer Station area (~64.04°S, 64.46°W), where studies of the species have been ongoing since 1974 (Fraser and Patterson 1997). Two events are especially noteworthy. The first concerns changes in breeding population numbers. Compared to the previous season, numbers decreased by 40% (7161 versus 4288 breeding pairs), which represents the largest between-year change in the long-term record (cf. Fraser and Patterson 1997; Smith et al. 2003a,b). The fact that numbers increased somewhat the following season (4288 versus 5635 breeding pairs) suggests that large numbers of birds deferred breeding. However, breeding pair numbers have not returned to pre-2001/02 levels, indicating that many birds were lost due to mortality. The second event concerns breeding success, or the number of chicks crêched per breeding pair. The long-term average for this region is 1.35, whereas during 2001/02 it was 0.78, the lowest reproductive success observed in the record. This was due primarily to deep spring snow accumulations and resulting meltwater, which flooded nests and drowned eggs and hatchlings. Peak fledging for the chicks that survived, moreover, occurred one week later relative to the long-term average (i.e., 12 February). This corresponded with an equal delay in peak egg laying, rather than with ensuing changes in krill abundance and availability. The latter are cyclical in the region, and while Adélie penguin foraging trip durations were indeed longer during 2001/02, they fell within the range of previously reported variability (Fraser and Hofmann 2003).

The region's Adélie penguin populations have been decreasing over the past three decades (Fraser and Patterson 1997; Patterson et al. 2003; Smith et al. 2003a,b). This is in response to increasing winter warming in the WAP, which has forced a decrease in sea ice availability (Fraser et al. 1992; Jacobs and Comiso 1997; Parkinson 2002; Smith and Stammerjohn 2001;

Vaughan et al. 2001) and an increase in precipitation (Thompson et al. 1994). Fraser and Trivelpiece (1996) discussed these changes in Adélie penguin populations within the context of a "habitat optimum" model and suggested that in this region habitat conditions have passed beyond the optimum required by Adélie penguin life history. The changes in breeding pairs and breeding success observed during 2001/02 suggest that adverse environmental conditions periodically breach critical life history thresholds from which populations do not recover. This would explain why Adélie penguin population trends in this region show a pattern of episodic, stepwise decreases with interim periods of relative population stability (cf. Fraser and Patterson 1997; Smith et al. 2003a,b), and highlights the importance of understanding life history strategies within the context of investigating linkages to climate change (Fraser and Trivelpiece 1996; Fraser and Hofmann 2003).

d. The hemispheric context

As shown earlier in Fig. 3, the anomalous atmospheric circulation around the Antarctic Peninsula from September 2001 through February 2002 was part of a circumpolar amplification of the mean wavenumber-3 pattern. This also had a major impact on other regions around Antarctica. For example, the combination of a blocking high in the South Atlantic and deep low pressure anomalies to the south created the heaviest austral-summer sea ice conditions in the southeast Weddell Sea in 2002 for at least 50 yr (Turner et al. 2002). The circumpolar anomaly pattern also resulted in unusual intrusions of midlatitude air into the continental ice sheet interior. The high pressure anomaly at ~110°E (in the South Tasman Sea and marked 3 in Fig. 3), another common location for blocking-high activity (Pook and Gibson 1999; Trenberth and Mo 1985), was indirectly responsible for periods of slight to moderate snowfall at Dome C in East Antarctica (74.5°S, 123.0°E; elevation 3280 m; Massom et al. 2004)—a rare event for this extremely dry region of the high interior ice sheet plateau. This episode also caused anomalously high surface wind speeds (snow redistribution) and air temperatures over the continental interior. On 11 January 2002, Vostok (78.5°S, 106.9°E; elevation 3488 m) experienced a temperature of –16.5°C, close to the record high of –13.3°C (on 6 January 1974), as reported by Turner et al. (2002). Similarly, South Pole station had a maximum temperature of –18.1°C and a peak wind speed of ~16.5 m s^{-1} on 11 January. The annual mean temperature is <-50°C in both locations, with calm conditions usually prevailing at this time of year. Farther to the west, the deep low pressure anomaly centered on southern Australia had a significant influence on the weather in that region, bringing anomalously cold and wet conditions in the austral summer of 2001/02.

6. Summary

An anomalous pattern of atmospheric circulation, dominated by strong, warm, and moisture-laden winds with a predominant northerly component, had an extreme effect across a wide area of the West (and East) Antarctic Peninsula region over a 5–6-month period in late 2001 to early 2002. This had a profound impact on regional sea ice and ocean conditions and marine ecology. This impact was highly complex, and indeed paradoxical, with counteractive processes occurring simultaneously. Specific conclusions of note include the following:

1) The anomalous atmospheric pattern in 2001/02, which Turner et al. (2002) attribute to natural variability and which coincided with a positive Southern Annular Mode index, transported warm air over a region that has been experiencing a significant warming trend over the past 55 yr (King 1994; Smith et al. 1999; Vaughan et al. 2003). Smith et al. (1999) note that the warming trend along the WAP has been strongest in midwinter (June) and suggest that this will affect the extent, concentration, and thickness of the sea ice, and therefore the associated marine ecology in agreement with our observations discussed herein. Large atmospheric anomalies of this kind are extremely rare (Turner et al. 2002), and the 2001/02 event was the most anomalous within the approximately 100-yr meteorological record at South Georgia. An important question remains as to whether blocking-high episodes, which tend to be abrupt and difficult to predict, will become more or less prevalent in a global-change scenario.
2) Sea ice dynamics were crucial to the development of the negative ice extent anomaly reported here, that is, an unusually early and rapid (short) retreat season (negative ice extent anomaly). Extreme ice compaction driven by strong winds with a dominant northerly component created an extraordinarily compact marginal ice zone, led to a major increase in ice thickness, deformation, and overrafting, and played a key role in the observed sea ice retreat. These results reinforce those of Turner et al. (2003)—of another rapid and large retreat in the Bellingshausen Sea in winter (of 1993) in which ice dynamics again dominated melt—but the compaction in 2001/02 crucially occurred over a much longer time period (October through February). Moreover, they build upon other studies, for ex-

ample, by Allison (1989) and Stammerjohn et al. (2003), which underline the importance of ice dynamics as a key determinant of Antarctic ice extent in certain sectors.

3) Furthermore, this ice compaction gave rise to more extensive ice with above-average ice concentrations near the coast throughout summer in 2002, that is, a sign change occurred in ice extent anomaly from negative to positive with the transition from spring to summer in 2001/02.
4) Because of the extreme over-rafted ice thickness, usual observational techniques for assessing ice thickness were inadequate. Standard ship observation and ice-drilling protocols yielded serious underestimates of the actual ice thickness (which was resolved by contemporary scuba diver observations). Furthermore, satellite estimates of sea ice extent alone represent an incomplete and at times oversimplistic indicator or descriptor of climate and/or ecological variability and change in that it fails to take account of the degree of ice compaction and accompanying dynamically driven changes in ice thickness and deformation. New satellite-derived estimates of sea ice thickness from CryoSat-2 (Drinkwater et al. 2005) and ICESat (Kwok et al. 2004) are important in this respect.
5) High snowfall under blizzard conditions resulted in a snow cover that was significantly thicker than the climatological mean. Resultant snow loading combined with enhanced ice deformation and an increase in ice permeability due to the warm conditions to cause widespread flooding of the snow–ice interface, resulting in enhanced snow–ice formation. Furthermore, persistently high temperatures caused widespread ice and snowmelt, which had a major impact on ice/snow microstructure and properties as well as on upper-ocean structure, that is, major freshening and stratification.
6) The complex conditions in 2001/02 likely had a major impact on snow and ice optical and microwave properties, with implications for the surface energy budget, ice–ocean–atmosphere feedback effects, phytoplankton growth, UVB penetration, and the unambiguous interpretation of satellite data.
7) An extensive and productive algal infiltration community formed in the relatively high illumination conditions of the ice surface in the spring of 2001 in response to (a) the warm conditions (with a large proportion of the ice cover exceeding the percolation threshold) and (b) a predominance of negative freeboards. Mechanical breakdown of this ice by wave–ice interaction in the marginal-ice zone gave rise to a strong intra-ice bloom in the early austral spring of 2001/02. As it initially occurred in the presence of a 100% (albeit unconsolidated) sea ice cover, the bloom was impossible to detect in satellite ocean color data alone. Indeed, analysis of SeaWiFS data shows that a strong negative anomaly occurred in chlorophyll concentration seaward of the ice edge in October 2001. Subsequently, this intra-ice community was followed by an anomalously high late spring/summer phytoplankton bloom in the WAP area. The implications are that the initial timing and distribution of sea ice–related algal blooms may go undetected from space when they occur within a compact sea ice zone. While the WAP region is known as an area of relatively high levels of sea ice algal production compared to other Antarctic sectors (Ackley and Sullivan 1994), the intense algal bloom in 2001 occurred relatively far to the south and unusually early in the season.
8) The relationship between krill (and other organisms) and sea ice in the WAP region is determined by more complex sea ice characteristics than ice extent alone. These include the degree of deformation as it affects over-rafting, and the temperature, snow cover, and flooding of the ice as they affect phytoplankton (prey) growth and distribution within the ice column. This is in agreement with earlier observations (Frazer et al. 1997) that sea ice structural characteristics appear to be the prime determinant of larval krill abundance and distribution in winter, with larval krill having an affinity for interstitial gaps between blocks of over-rafted ice. On the other hand, negative growth appears to have occurred in larval krill over this period—possibly a negative impact of the anomalously heavy ice conditions.
9) Adélie penguins, a regional top predator, experienced the largest recorded between-season breeding population decrease and lowest reproductive success in a 30-yr time series. Causal factors included nest flooding and drowning of eggs and small chicks due to snowmelt, and sea ice conditions that forced large numbers of birds to defer breeding and may also have induced winter mortality.
10) The degree of sea ice compaction is a key factor affecting the ability of apex predators to locate and access prey and air to breath and to haul out. Here, we show the importance of distinguishing between ice extent and "heaviness" (that accounts for ice thickness/degree of deformation and compaction), because of the latter's great ecological importance. What made the situation ecologically extraordinary in 2001/02 was the sheer persistence of the com-

bined ice convergence, melt, and heavy snowfall over a period of 5–6 months. Moreover, the major ecological impact persisted through summer, with very heavy ice cover remaining in a region that is generally ice free. Consequently, these events influenced all trophic levels within the WAP marine ecosystem.

Variability related to blocking-high events has significant implications, given the key role that sea ice plays in the global climate system by influencing the regional heat budget, surface albedo, and consequently oceanic and atmospheric circulation. This and other factors outlined in this paper are testament to the highly complex impacts discussed above and underline the critical need for further research.

Acknowledgments. The authors acknowledge the magnificent support of Captain Joe Borkowski and the crew of the R/V *Nathaniel B. Palmer* under very difficult conditions. The work was carried out on NSF Grant OPP-0084324 (CF) and NSF Palmer LTER Grant OPP96-32763, and the support of NSF is gratefully acknowledged. For RM, this work was supported by the Australian Government's Cooperative Research Centres Programme through the Antarctic Climate and Ecosystems Cooperative Research Centre (ACE CRC). The following cruise participants are gratefully acknowledged: the krill study dive team (Tim Newberger, Charlie Boch, Jordan Watson, and Jenny White) for underwater ice photography and krill information; Andy Ross (Oregon State University) for nutrient analysis; Jeff Otten (Raytheon) for collection and processing of TeraScan satellite data; Wendy Kozlowski, Karie Sines, Karen Pelletreau, Irene Garibotti, and Pamela Yeh for biological data collection and sample analysis; Raul Guerrero for CTD data collection; and Enrique Curchister for snow, optics, and sea ice data collection. The MPC Randy Sliester and the Raytheon support staff, Mo Hodgkins, Matt Burke, and Stian Allesandrini, Roman Botko, Kevin Bliss, and Julianne Lamsek, are thanked for their excellent support. Grateful thanks are also given to Hajo Eicken (University of Alaska) for useful discussions on ice basal growth processes. NCEP–NCAR reanalysis data were acquired from NOAA via http://www.cdc.noaa.gov/cdc/reanalysis/reanalysis.shtml. Meteorological data from Rothera Station were obtained from the British Antarctic Survey at http://www.antarctica.ac.uk/cgi-bin/metdb-form-2.pl?tabletouse=U_MET.ROTHERA_SYNOP&complex=1&idmask=.....&acct=cmet. SAM index data were obtained from Gareth Marshall (BAS) at http://www.nerc-bas.ac.uk/icd/gjma/sam.html. SSM/I ice concentration data were obtained from the NASA Earth Observing System Distributed Active Archive Center (DAAC) at the U.S. National Snow and Ice Data Center, University of Colorado, Boulder (http://nsidc.org). SSM/I-derived maps of sea ice motion were supplied by Chuck Fowler (University of Colorado). (SeaWiFS data were obtained online at http://oceancolor.gsfc.nasa.gov). AVHRR mosaics were obtained from the University of Wisconsin Space Science and Engineering Center (http://www.ssec.wisc.edu/). This paper benefited greatly from the input of three anonymous reviewers and Dr. Gudrun Magnusdottir (editor of *Journal of Climate*).

REFERENCES

Ackley, S. F., and C. W. Sullivan, 1994: Physical controls on the development and characteristics of Antarctic sea ice biological communities—A review and synthesis. *Deep-Sea Res.,* **41,** 1583–1604.

Allison, I., 1989: Pack-ice drift off East Antarctica. *Ann. Glaciol.,* **12,** 1–8.

Arrigo, K. R., D. L. Worthen, M. P. Lizotte, P. Dixon, and G. Dieckmann, 1997: Primary production in Antarctic sea ice. *Science,* **276,** 394–397.

Beardsley, R. C., R. Limeburner, and W. Brechner Owens, 2004: Drifter measurements of surface currents near Marguerite Bay on the West Antarctic Peninsula shelf during austral summer and fall, 2001 and 2002. *Deep-Sea Res.,* **51B,** 1947–1964.

Carleton, A. M., 2003: Atmospheric teleconnections involving the Southern Ocean. *J. Geophys. Res.,* **108,** 8080, doi:10.1029/2000JC000379.

Chapman, E. W., C. A. Ribic, and W. R. Fraser, 2004: The distribution of seabirds and pinnepeds in Marguerite Bay and their relationship to physical features during austral winter 2001. *Deep-Sea Res.,* **51B,** 2261–2278.

Colbeck, S. C., 1982: An overview of seasonal snow metamorphism. *Rev. Geophys.,* **29,** 81–96.

Comiso, J. C., 1995: SSM/I ice concentrations using the Bootstrap algorithm. NASA Rep. 1380, NASA Goddard Space Flight Center, Greenbelt, MD, 40 pp.

Connolley, W. M., 2003: Long-term variation of the Antarctic Circumpolar Wave. *J. Geophys. Res.,* **108,** 8076, doi:10.1029/2000JC000380.

Dierssen, H. M., and R. C. Smith, 2000: Bio-optical properties and remote sensing ocean color algorithms for Antarctic Peninsula Waters. *J. Geophys. Res.,* **105** (C11), 26 301–26 312.

Drinkwater, M. R., R. Francis, G. Ratier, and D. Wingham, 2005: The European Space Agency's Earth Explorer Mission CryoSat: Measuring variability in the cryosphere. *Ann. Glaciol.,* **39,** 313–320.

Eicken, H., 1998: Deriving modes and rates of ice growth in the Weddell Sea from microstructural, salinity and stable-isotope data. *Antarctic Sea Ice Physical Properties and Processes,* M. O. Jeffries, Ed., Amer. Geophys. Union, 89–122.

——, H. Fischer, and P. Lemke, 1995: Effects of the snow cover on Antarctic sea ice and potential modulation of its response to climate change. *Ann. Glaciol.,* **21,** 369–376.

——, H. R. Krouse, D. Kadko, and D. K. Perovich, 2002: Tracer studies of pathways and rates of meltwater transport through

Arctic summer sea ice. *J. Geophys. Res.,* **107,** 8046, doi:10.1029/2000JC000583.

Emery, W. J., C. W. Fowler, and J. A. Maslanik, 1997: Satellite-derived maps of Arctic and Antarctic sea ice motions: 1988–1994. *Geophys. Res. Lett.,* **24,** 897–900.

Enomoto, H., and A. Ohmura, 1990: The influences of atmospheric half-yearly cycle on sea ice extent in the Antarctic. *J. Geophys. Res.,* **95,** 9497–9511.

Fichefet, T., and M. A. Morales Maqueda, 1999: Modelling the influence of snow accumulation and snow-ice formation on the seasonal cycle of the Antarctic sea-ice cover. *Climate Dyn.,* **15,** 251–268.

Fraser, W. R., and W. Z. Trivelpiece, 1996: Factors controlling the distribution of seabirds: Winter-summer heterogeneity in the distribution of Adélie penguin populations. *Foundations for Ecological Research West of the Antarctic Peninsula,* R. M. Ross, E. Hofmann, and L. B. Quetin, Eds., Amer. Geophys. Union, 257–272.

——, and D. L. Patterson, 1997: Human disturbance and long-term changes in Adélie penguin populations: A natural experiment at Palmer Station, Antarctic Peninsula. *Antarctic Communities: Species, Structure and Survival,* B. Battaglia, J. Valencia, and D. W. H. Walton, Eds., Cambridge University Press, 445–452.

——, and E. E. Hofmann, 2003: A predator's perspective on causal links between climate change, physical forcing and ecosystem response. *Mar. Ecol. Prog. Ser.,* **265,** 1–15.

——, W. Z. Trivelpiece, D. G. Ainley, and S. G. Trivelpiece, 1992: Increase in Antarctic penguin populations: Reduced competition with whales or a loss of sea ice due to environmental warming? *Polar Biol.,* **11,** 525–531.

Frazer, T. K., L. B. Quetin, and R. M. Ross, 1997: Abundance and distribution of larval krill, *Euphausia superba,* associated with annual sea ice in winter. *Antarctic Communities: Species, Structure and Survival,* B. Battaglia, J. Valencia, and D. W. H. Walton, Eds., Cambridge University Press, 107–111.

Fritsen, C. H., J. N. Kremer, S. F. Ackley, and C. W. Sullivan, 1998: Flood-freeze cycles and algal dynamics in Antarctic pack ice. *Antarctic Sea Ice: Biological Processes,* M. L. Lizotte and K. R. Arrigo, Eds., Amer. Geophys. Union, 1–21.

Fyfe, J. C., G. J. Boer, and G. M. Flato, 1999: The Arctic and Antarctic Oscillations and their projected changes under global warming. *Geophys. Res. Lett.,* **26,** 1601–1604.

Gillett, N. P., and D. W. J. Thompson, 2003: Simulation of recent Southern Hemisphere climate change. *Science,* **302,** 273–275.

Gloersen, P., 1995: Modulation of hemispheric sea ice cover by ENSO events. *Nature,* **373,** 503–506.

——, W. J. Campbell, D. J. Cavalieri, J. C. Comiso, C. L. Parkinson, and H. J. Zwally, 1992: Arctic and Antarctic Sea Ice, 1978–1987: Satellite Passive Microwave Observations and Analysis, NASA Special Publication SP-511, 290 pp.

Golden, K. M., S. F. Ackley, and V. I. Lytle, 1998: The percolation phase transition in sea ice. *Science,* **282,** 2238–2241.

Hall, A., and M. Visbeck, 2002: Synchronous variability in the Southern Hemisphere atmosphere, sea ice, and ocean resulting from the annular mode. *J. Climate,* **15,** 3043–3057.

Hanson, A. M., 1965: Studies of the mass budget of Arctic pack-ice floes. *J. Glaciol.,* **5,** 701–709.

Harangozo, S. A., 1997: Atmospheric meridional circulation impacts on contrasting winter sea ice extent in two years in the Pacific sector of the Southern Ocean. *Tellus,* **49,** 388–400.

——, 2000: A search for ENSO teleconnections in the west Antarctic Peninsula climate in austral winter. *Int. J. Climatol.,* **20,** 663–679.

——, 2004: The impact of winter ice retreat on Antarctic winter sea ice extent and links to atmospheric meridional circulation. *Int. J. Climatol.,* **24,** 1023–1044.

Hines, K. M., D. H. Bromwich, and G. J. Marshall, 2000: Artificial surface pressure trends in the NCEP–NCAR reanalysis over the Southern Ocean and Antarctica. *J. Climate,* **13,** 3940–3952.

Horner, R., and Coauthors, 1992: Ecology of sea ice biota. 1. Habitat, terminology, and methodology. *Polar Biol.,* **12,** 417–427.

Hurrell, J. W., and H. van Loon, 1994: A modulation of the atmospheric annual cycle in the Southern Hemisphere. *Tellus,* **46A,** 325–338.

Jacobs, S. S., and J. C. Comiso, 1997: Climate variability in the Amundsen and Bellingshausen Seas. *J. Climate,* **10,** 697–709.

Jeffries, M. O., and U. Adolphs, 1997: Early winter snow and ice thickness distribution, ice structure and development of the western Ross Sea pack ice between the ice edge and the Ross Ice Shelf. *Antarct. Sci.,* **9,** 188–200.

——, R. A. Shaw, K. Morris, A. L. Veazey, and H. R. Krouse, 1994a: Crystal structure, stable isotopes (δ18O) and development of sea ice in the Ross, Amundsen and Bellingshausen Seas. *J. Geophys. Res.,* **99** (C1), 985–995.

——, A. L. Veazey, K. Morris, and H. R. Krouse, 1994b: Depositional environment of the snow cover on West Antarctic pack-ice floes. *Ann. Glaciol.,* **20,** 33–38.

——, S. Li, R. A. Jaña, H. R. Krouse, and B. Hurst-Cushing, 1998: Late winter first-year ice floe thickness variability, seawater flooding and snow ice formation in the Amundsen and Ross Seas. *Antarctic Sea Ice Physical Processes, Interactions and Variability,* M. O. Jeffries, Ed., Amer. Geophys. Union, 69–88.

Johnson, K. S., R. L. Petty, and J. Tomsen, 1985: Flow injection analysis in seawater macronutrients. *Mapping Strategies in Chemical Oceanography,* A. Zirino, Ed., Advances in Chemistry Series, Vol. 209, American Chemical Society, 7–30.

Kadko, D., 2000: Modeling the evolution of the Arctic mixed layer during the fall, 1997 Surface Heat Budget of the Arctic Ocean (SHEBA) Project using measurements of 7Be. *J. Geophys. Res.,* **105,** 3369–3378.

Kalnay, E., and Coauthors, 1996: The NCEP/NCAR 40-Year Reanalysis Project. *Bull. Amer. Meteor. Soc.,* **77,** 437–471.

Karoly, D. J., 1990: The role of transient eddies in low frequency zonal variations of the Southern Hemisphere circulation. *Tellus,* **42A,** 41–50.

Kidson, J. W., 1988: Interannual variations in Southern Hemisphere circulation. *J. Climate,* **1,** 1177–1198.

——, 1999: Principal modes of Southern Hemisphere low-frequency variability obtained from NCEP–NCAR reanalyses. *J. Climate,* **12,** 2808–2830.

King, J. C., 1994: Recent climate variability in the vicinity of the Antarctic Peninsula. *Int. J. Climatol.,* **14,** 357–369.

——, and J. Turner, 1997: *Antarctic Meteorology and Climatology.* Cambridge University Press, 409 pp.

——, and S. A. Harangozo, 1998: Climate change in the western Antarctic Peninsula since 1945: Observations and possible causes. *Ann. Glaciol.,* **27,** 571–575.

——, and J. C. Comiso, 2003: The spatial coherence of interannual temperature variations in the Antarctic Peninsula. *Geophys. Res. Lett.,* **30,** 1040, doi:10.1029/2002GL015580.

Klinck, J. M., E. E. Hofmann, R. C. Beardsley, B. Salihoglu, and

S. Howard, 2004: Water-mass properties and circulation on the west Antarctic Peninsula continental shelf in austral fall and winter 2001. *Deep-Sea Res.,* **51B,** 1925–1946.

Kwok, R., and J. C. Comiso, 2002a: Southern Ocean climate and sea ice anomalies associated with the Southern Oscillation. *J. Climate,* **15,** 487–501.

——, and J. C. Comiso, 2002b: Spatial patterns of variability in Antarctic surface temperature: Connections to the Southern Hemisphere Annular Mode and the Southern Oscillation. *Geophys. Res. Lett.,* **29,** 1705, doi:10.1029/2002GL015415.

——, H. J. Zwally, and D. Yi, 2004: ICESat observations of Arctic sea ice: A first look. *Geophys. Res. Lett.,* **31,** L16401, doi:10.1029/2004GL020309.

Lange, M. A., P. Schlosser, S. F. Ackley, P. Wadhams, and G. S. Dieckmann, 1990: 18O concentrations in sea ice of the Weddell Sea, Antarctica. *J. Glaciol.,* **36** (124), 315–323.

Lejenäs, H., 1984: Characteristics of Southern Hemisphere blocking as determined from a time series of observational data. *Quart. J. Roy. Meteor. Soc.,* **110,** 967–979.

Liu, J., D. G. Martinson, X. Yuan, and D. Rind, 2002a: Evaluating simulated Antarctic sea ice variability and its global teleconnections in global climate models. *Int. J. Climatol.,* **22,** 885–900.

——, X. Yuan, D. Rind, and D. G. Martinson, 2002b: Mechanism study of the ENSO and southern high latitude climate teleconnections. *Geophys. Res. Lett.,* **29,** 1679, doi:1029/2002GL015143.

——, J. A. Curry, and D. G. Martinson, 2004: Interpretation of recent Antarctic sea ice variability. *Geophys. Res. Lett.,* **31,** L02205, doi:10.1029/2003GL018732.

Marshall, G. J., and S. A. Harangozo, 2000: An appraisal of NCEP/NCAR reanalysis MSLP data viability for climate studies in the South Pacific. *Geophys. Res. Lett.,* **27,** 3057–3060.

Massom, R. A., and Coauthors, 2001: Snow on Antarctic sea ice. *Rev. Geophys.,* **39,** 413–445.

——, M. J. Pook, J. C. Comiso, N. Adams, J. Turner, T. Lachlan-Cope, and T. Gibson, 2004: Precipitation over the interior East Antarctic Ice Sheet related to midlatitude blocking-high activity. *J. Climate,* **17,** 1914–1928.

Meehl, G. A., J. W. Hurrell, and H. van Loon, 1998: A modulation of the mechanism of the semi-annual oscillation in the Southern Hemisphere. *Tellus,* **50A,** 442–450.

Menendez, C. G., V. Serafini, and H. Le Treut, 1999: The storm tracks and energy cycle of the Southern Hemisphere: Sensitivity to sea-ice boundary conditions. *Ann. Geophys.,* **17,** 1478–1492.

Meredith, M. P., I. A. Renfrew, A. Clarke, J. C. King, and M. A. Brandon, 2004: Impact of the 1997/98 ENSO on the upper waters of Marguerite Bay, western Antarctic Peninsula. *J. Geophys. Res.,* **109,** C09013, doi:10.1029/2003JC001784.

Murray, R. J., and I. Simmonds, 1995: Responses of climate and cyclones to reductions in Arctic winter sea ice. *J. Geophys. Res.,* **100,** 4791–4806.

Nansen, F., 1902: The oceanography of the North Polar Basin. *The Norwegian North Polar Expedition 1893–1896, Scientific Results,* Vol. 3, No. 9, Longmans, Green, and Co., 427 pp.

Notz, D., M. G. McPhee, M. G. Worster, G. A. Maykut, K. H. Schlünzen, and H. Eicken, 2003: Impact of underwater-ice evolution on Arctic summer sea ice. *J. Geophys. Res.,* **108,** 3223, doi:10.1029/2001JC001173.

O'Reilly, J. E., S. Maritorena, B. G. Mitchell, D. A. Siegel, K. L. Carder, S. A. Garver, M. Kahru, and C. McClain, 1998: Ocean color chlorophyll algorithms for SeaWiFS. *J. Geophys. Res.,* **103** (C11), 24 937–24 953.

Parkinson, C., 2002: Trends in the length of the Southern Ocean sea-ice season, 1979–99. *Ann. Glaciol.,* **34,** 435–440.

Patterson, D. L., A. Easter-Pilcher, and W. R. Fraser, 2003: The effects of human activity and environmental variability on long-term changes in Adélie penguin populations at Palmer Station, Antarctica. *Antarctic Biology in a Global Context: Scientific Committee for Antarctic Research (SCAR), Eighth Biological Symposium,* A. H. L. Huiskes et al., Eds., Backhuys Publishers, 301–307.

Perovich, D. K., 1996: The optical properties of sea ice. CRREL Rep. 96-1, Cold Regions Research and Engineering Laboratory, Hanover, NH, 25 pp.

——, T. C. Grenfell, J. A. Richter-Menge, B. Light, W. B. Tucker III, and H. Eicken, 2003: Thin and thinner: Ice mass balance measurements during SHEBA. *J. Geophys. Res.,* **108,** 8050, doi:10.1029/2001JC001079.

——, B. C. Elder, K. J. Claffey, S. E. Stammerjohn, R. C. Smith, S. F. Ackley, H. R. Krouse, and A. J. Gow, 2004: Winter sea-ice properties in Marguerite Bay, Antarctica. *Deep-Sea Res.,* **51B,** 2023–2039.

Pook, M., and T. Gibson, 1999: Atmospheric blocking and storm tracks during SOP-1 of the FROST Project. *Aust. Meteor. Mag.* (Special Edition), 51–60.

Quetin, L. B., and R. M. Ross, 1991: Behavioral and physiological characteristics of the Antarctic krill, *Euphausia superba. Amer. Zool.,* **31,** 49–63.

——, and ——, 2001: Environmental variability and its impact on the reproductive cycle of Antarctic krill. *Amer. Zool.,* **41,** 74–89.

——, and ——, 2003: Episodic recruitment in Antarctic krill, *Euphausia superba,* in the Palmer LTER study region. *Mar. Ecol. Prog. Ser.,* **259,** 185–200.

——, ——, R. C. Smith, W. Z. Trivelpiece, and M. Vernet, 1996: The Palmer LTER Group: The western Antarctic Peninsula region: Summary of environmental and ecological processes. *Foundations for Ecological Research West of the Antarctic Peninsula,* R. M. Ross, E. Hofmann, and L. B. Quetin, Eds., Amer. Geophys. Union, 437–448.

——, ——, T. K. Frazer, M. O. Amsler, C. Wyatt-Evens, and S. A. Oakes, 2003: Growth of larval krill, *Euphausia superba,* in fall and winter west of the Antarctic Peninsula. *Mar. Biol.,* **143,** 833–843.

Raphael, M. N., 2003: Impact of observed sea-ice concentration on the Southern Hemisphere extratropical atmospheric circulation in summer. *J. Geophys. Res.,* **108,** 4687, doi:10.1029/2002JD003308.

Ross, R. M., E. E. Hofmann, and L. B. Quetin, 1996: *Foundations for Ecological Research West of the Antarctic Peninsula*. Amer. Geophys. Union, 448 pp.

——, L. B. Quetin, T. Newberger, and S. A. Oakes, 2004: Growth and behavior of larval krill (*Euphausia superba*) under the ice in late winter 2001 west of the Antarctic Peninsula. *Deep-Sea Res.,* **51B,** 2169–2184.

Simmonds, I., 2003: Modes of atmospheric variability over the Southern Ocean. *J. Geophys. Res.,* **108,** 8078, doi:10.1029/2000JC000542.

——, and T. H. Jacka, 1995: Relationships between the interannual variability of Antarctic sea ice and the Southern Oscillation. *J. Climate,* **8,** 637–647.

——, and K. Keay, 2000: Variability of Southern Hemisphere

extratropical cyclone behavior, 1958–97. *J. Climate,* **13,** 550–561.

——, and J. C. King, 2004: Global and hemispheric climate variations affecting the Southern Ocean. *Antarct. Sci.,* **16,** 401–413.

Sinclair, M. R., 1996: A climatology of anticyclones and blocking for the Southern Hemisphere. *Mon. Wea. Rev.,* **124,** 245–263.

Smith, R. C., and S. E. Stammerjohn, 2001: Variations of surface air temperature and sea ice extent in the western Antarctic Peninsula (WAP) region. *Ann. Glaciol.,* **33,** 493–500.

——, K. S. Baker, and P. Dustan, 1981: Fluorometric techniques for the measurement of oceanic chlorophyll in the support of remote sensing. Scripps Institution of Oceanography Reference 81-17, Visibility Laboratory, Scripps Institute of Oceanography, University of California, 14 pp.

——, and Coauthors, 1995: The Palmer LTER: A long-term ecological research program at Palmer Station, Antarctica. *Oceanography,* **8** (3), 77–86.

——, S. E. Stammerjohn, and K. S. Baker, 1996: Surface air temperature variations in the Western Antarctic Peninsula region. *Foundations for Ecological Research West of the Antarctic Peninsula,* R. M. Ross, E. Hofmann, and L. B. Quetin, Eds., Amer. Geophys. Union, 105–121.

——, and Coauthors, 1999: Marine ecosystem sensitivity to climate change. *Bioscience,* **49,** 393–404.

——, W. R. Fraser, and S. E. Stammerjohn, 2003a: Climate variability and ecological response of the marine ecosystem in the western Antarctic Peninsula (WAP) region. *Climate Variability and Ecosystem Response at Long-Term Ecological Research (LTER) Sites,* D. Greenland, D. G. Goodin, and R. C. Smith, Eds., Oxford University Press, 158–173.

——, ——, ——, and M. Vernet, 2003b: Palmer Long-Term Ecological Research on the Antarctic marine ecosystem. *Antarctic Peninsula Climate Variability: Historical and Paleoenvironmental Perspectives,* E. W. Domack et al., Eds., Amer. Geophys. Union, 131–144.

Smith, W. O., and D. M. Nelson, 1985: Phytoplankton bloom produced by a receding ice edge in the Ross Sea: Spatial coherence with the density field. *Science,* **227,** 163–166.

Stammerjohn, S. E., and R. C. Smith, 1996: Spatial and temporal variability in Western Antarctic Peninsula sea ice coverage. *Foundations for Ecological Research West of the Antarctic Peninsula,* R. M. Ross, E. E. Hofmann, and L. B. Quetin, Eds., Amer. Geophys. Union, 81–104.

——, and ——, 1997: Opposing Southern Ocean climate patterns as revealed by trends in sea ice coverage. *Climate Change,* **37,** 617–639.

——, M. R. Drinkwater, R. C. Smith, and X. Liu, 2003: Ice-atmosphere interactions during sea-ice advance and retreat in the western Antarctic Peninsula region. *J. Geophys. Res.,* **108,** 3329, doi:10.1029/2002JC001543.

Thompson, D. W. J., and J. M. Wallace, 2000: Annular modes in extratropical circulation. Part I: Month-to-month variability. *J. Climate,* **13,** 1018–1036.

——, and S. Solomon, 2002: Interpretation of recent Southern Hemisphere climate change. *Science,* **296,** 895–899.

——, J. M. Wallace, and G. C. Hegeri, 2000: Annular modes in extratropical circulation. Part II: Trends. *J. Climate,* **13,** 1000–1016.

Thompson, L. G., D. A. Peel, E. Mosley-Thompson, R. Mulvaney, J. Dai, P. N. Lin, M. E. Davis, and C. F. Raymond, 1994: Climate since A.D. 1510 on Dyer Plateau, Antarctic Peninsula: Evidence for recent climate change. *Ann. Glaciol.,* **20,** 420–426.

Trenberth, K. E., and K. C. Mo, 1985: Blocking in the Southern Hemisphere. *Mon. Wea. Rev.,* **113,** 3–21.

Turner, J., 2004: The El Niño-Southern Oscillation and Antarctica. *Int. J. Climatol.,* **24,** 1–31.

——, S. A. Harangozo, G. J. Marshall, J. C. King, and S. R. Colwell, 2002: Anomalous atmospheric circulation over the Weddell Sea, Antarctica, during the austral summer of 2001/02 resulting in extreme sea-ice conditions. *Geophys. Res. Lett.,* **29,** 2160, doi:10.1029/2002GL015565.

——, ——, J. C. King, W. M. Connolley, T. A. Lachlan-Cope, and G. J. Marshall, 2003: An exceptional winter sea-ice retreat/advance in the Bellingshausen Sea, Antarctica. *Atmos.–Ocean,* **41,** 171–185.

——, and Coauthors, 2004: Antarctic climate change during the last 50 years. *Int. J. Climatol.,* **25,** 279–294.

Van den Broecke, M. R., 1998: The semi-annual oscillation and Antarctic climate, part 2: Recent changes. *Antarct. Sci.,* **10,** 184–191.

van Loon, H., 1956: Blocking action in the Southern Hemisphere. Part 1. *Notos,* **5,** 171–175.

Vaughan, D. G., G. J. Marshall, W. M. Connolley, J. C. King, and R. Mulvaney, 2001: Climate change—Devil in the detail. *Science,* **293,** 1777–1779.

——, and Coauthors, 2003: Recent rapid regional climate warming on the Antarctic Peninsula. *Climate Change,* **60,** 243–274.

Warren, S. G., 1982: The optical properties of snow. *Rev. Geophys. Space Phys.,* **20,** 67–89.

Watkins, A. B., and I. Simmonds, 1999: Late spring surge in the open water of the Antarctic sea ice pack. *Geophys. Res. Lett.,* **26,** 1481–1484.

White, W. B., and R. G. Peterson, 1996: An Antarctic circumpolar wave in surface pressure, wind, temperature and sea ice extent. *Nature,* **380,** 699–702.

——, C. Shyh-Chin, R. J. Allan, and R. C. Stone, 2002: Positive feedbacks between the Antarctic Circumpolar Wave and the global El Niño-Southern Oscillation Wave. *J. Geophys. Res.,* **107,** 3165, doi:10.1029/2000JC000581.

Worby, A. P., and I. Allison, 1999: A ship-based technique for observing Antarctic sea ice. Part I: Observational techniques and results. Antarctic CRC Rep. 15, Antarctic Cooperative Research Centre, University of Tasmania, 23 pp.

——, M. O. Jeffries, W. F. Weeks, K. Morris, and R. Jaña, 1996: The thickness distribution of sea ice and snow cover during late winter in the Bellingshausen and Amundsen Seas. *J. Geophys. Res.,* **101** (C12), 28 441–28 455.

Wright, A. D. F., 1974: Blocking action in the Australian region. Tech. Rep. 10, Australian Bureau of Meteorology, 29 pp.

Wu, X., W. F. Budd, V. I. Lytle, and R. A. Massom, 1999: The effect of snow on Antarctic sea ice simulations in a coupled atmosphere-sea ice model. *Climate Dyn.,* **15,** 127–143.

Yuan, X., 2004: ENSO-related impacts on Antarctic sea ice: A synthesis of phenomenon and mechanisms. *Antarct. Sci.,* **16,** 415–425.

——, and D. G. Martinson, 2000: Antarctic sea ice variability and its global connectivity. *J. Climate,* **13,** 1697–1717.

——, and ——, 2001: The Antarctic Dipole and its predictability. *Geophys. Res. Lett.,* **28,** 3609–3612.

Zwally, H. J., J. C. Comiso, C. L. Parkinson, D. J. Cavalieri, and P. Gloersen, 2002: Variability of Antarctic sea ice 1979–1998. *J. Geophys. Res.,* **107,** 3041, doi:10.1029/2000JC000733.